

AD-A065 942

H S S INC BEDFORD MASS

EOMET-77. ATMOSPHERIC TRANSMISSION VALUES DERIVED FROM PHOTOGRA--ETC(U)

DEC 78 H S STEWART, M P SHULER, L B WOOLAVER

N00173-78-C-0160

F/G 4/1

NL

UNCLASSIFIED

HSS-B-049

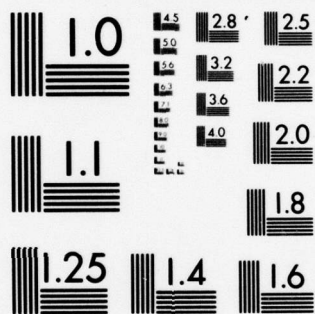
1 OF 1
AD
A065942



END
DATE
FILMED

5-79

DDC



MICROCOPY RESOLUTION TEST CHART
NATIONAL BUREAU OF STANDARDS-1963-A

AD A0 65942

DDC FILE COPY

LEVEL

HSS-B-049

12

EOMET-77
ATMOSPHERIC TRANSMISSION VALUES DERIVED
FROM PHOTOGRAPHS OF THE SEA HORIZON (U)

HSS Inc
2 Alfred Circle
Bedford, Ma 01730

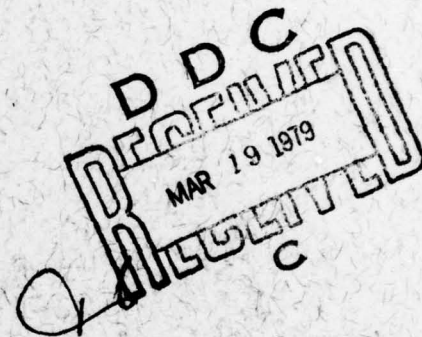
H. S. Stewart
M. P. Shuler, Jr
L. B. Woolaver

28 December 1978

Final Report On Contract

N00173-78-C-0160

78 Jul 17 -- 79 Jan 31



Prepared For:

NAVAL RESEARCH LABORATORIES
Washington, D. C. 20375
Code: 8327

This document has been approved
for public release and sale; its
distribution is unlimited.

390 794

79 02 26 002

UNCLASSIFIED

SECURITY CLASSIFICATION OF THIS PAGE (When Data Entered)

REPORT DOCUMENTATION PAGE		READ INSTRUCTIONS BEFORE COMPLETING FORM
1. REPORT NUMBER	2. GOVT ACCESSION NO.	3. RECIPIENT'S CATALOG NUMBER
6. TITLE (and Subtitle) EOMET-77. Atmospheric Transmission Values Derived From Photographs of the Sea Horizon		5. TYPE OF REPORT & PERIOD COVERED Final Report , 78 Jul 17 - 79 Jan 31
7. AUTHOR H. S./Stewart, M. P./Shuler, Jr. L. B./Woolaver		8. PERFORMING ORG. REPORT NUMBER HSS-B-049
9. PERFORMING ORGANIZATION NAME AND ADDRESS HSS Inc 2 Alfred Circle Bedford, Mass 01730		10. PROGRAM ELEMENT, PROJECT, TASK AREA & WORK UNIT NUMBERS 17X4912, 1403 000 77777 000173 2F 000000 00
11. CONTROLLING OFFICE NAME AND ADDRESS Naval Research Laboratories Code 8327 Washington, D. C. 20375		12. REPORT DATE 28 December 1978
14. MONITORING AGENCY NAME & ADDRESS (if different from Controlling Office) 9. Final rept. 17 Jul 78 - 31 Jan 79		13. NUMBER OF PAGES 67
16. DISTRIBUTION STATEMENT (of this Report) 1269p.		15. SECURITY CLASS. (of this report) UNCLASSIFIED
17. DISTRIBUTION STATEMENT (of the abstract entered in Block 20, if different from Report) DISTRIBUTION STATEMENT A Approved for public release Distribution Unlimited		15a. DECLASSIFICATION/DOWNGRADING SCHEDULE N/A
18. SUPPLEMENTARY NOTES		
19. KEY WORDS (Continue on reverse side if necessary and identify by block number)		
20. ABSTRACT (Continue on reverse side if necessary and identify by block number)		

79 02 26 002

DD FORM 1 JAN 73 1473

EDITION OF 1 NOV 65 IS OBSOLETE

UNCLASSIFIED

SECURITY CLASSIFICATION OF THIS PAGE (When Data Entered)

390794

LB

TABLE OF CONTENTS

<u>Section</u>	<u>Page</u>
Table of Contents	1
List of Illustrations	2
List of Tables	3
1. INTRODUCTION	4
2. THEORY	6
3. DATA REDUCTION	19
4. DISCUSSION	27
5. CONCLUSIONS	29
REFERENCES	30
APPENDIX A	31
DISTRIBUTION	67

ACCESSION for

NTIS ☒ White Section

DOC ☐ Buff Section

the sample

A

LIST OF ILLUSTRATIONS

<u>Figure No.</u>	<u>Legend</u>	<u>Page</u>
1	Geometry of the Problem	7
2	Comparison of Geometric Solution to Bowditch	13
3	Effects of error in assumed position of horizon	17
4	Scanning Track of Photographs	20
5	Values of relative exposure from horizon trace	21
6-40	Detail Data Management -Appendix A	32

LIST OF TABLES

<u>Table No.</u>	<u>Legend</u>	<u>Page</u>
1	Error Analysis	15
2	Values of Scattering Coefficient, km^{-1}	25
3	Physical and Meteorological Conditions	27

EOMET '77

Atmospheric Transmission Values Derived from Photographs of the Sea Horizon

1. INTRODUCTION

1.1 There is limited experimental evidence that the transmission of the atmosphere at sea during the daytime can be deduced from photographs of the horizon.^{1,2} The experiments which have been reported result in reasonable values of transmission, but no separate measurement of transmission or transmission-related values have been made concurrent with the horizon photographs to demonstrate that the technique is valid.

1.2 The 1977 EOMET Cruise presented an opportunity to compare the results of horizon photographs with concurrently measured or recorded meteorological data such as visibility, aerosol concentration and size distribution, nephelometer readings etc. To test the techniques and implement such comparisons, groups of horizon photographs were made on twenty occasions between May 17 and June 6, 1977.

1.3 One photograph from each of the twenty groups has been selected by visual inspection to be most promising for data reduction. In addition, a properly exposed but challenging photograph has been selected from ten of the groups. Challenge includes cloud shadows, wind streaks, and white caps.

1.4 The horizon photographs were made with color film, and data reduction on a particular film results in three values of atmospheric

scattering coefficient, one in the blue centering on $\lambda_B = 0.44\mu$, one in the green with $\lambda_G = 0.55\mu$ and one in the red at $\lambda_R = 0.64\mu$. The coefficients are appropriate for the sum of molecular and aerosol scattering. Since molecular coefficients are known the aerosol scattering coefficients can be obtained if the method is valid.

1.5 → The end product of this report is a tabulation of aerosol scattering coefficients at three wavelengths obtained from color photographs of the horizon taken on twenty occasions during the 1977 cruise of the USNS Hayes. In addition, challenging photographs from ten occasions have been analyzed and the scattering coefficients obtained from them are compared with coefficients obtained from the corresponding most promising photographs. Pertinent supporting data are also presented. This includes date, time of day, latitude, longitude, wind direction, ship heading, and cloud type and cover.

2. THEORY

2.1 Equations for the apparent radiance of the sea at and near the horizon are developed here. The equations show the relationship between apparent radiance and atmospheric scattering coefficient. In particular, if photographs of the sea horizon are taken from a known altitude above sea level then relative radiance values extracted from the photographs may be used to calculate scattering coefficients.

2.2 Figure 1 illustrates the observing conditions. In the figure, ρ is the radius of the earth, R is the distance to the point observed on the sea surface, h is the height of the observer, θ is the depression from the horizontal of the line to the horizon and $\theta + \phi$ is the depression from the horizontal of the point observed. In what follows equations are developed for the apparent radiance of the path from the observer to any point on the sea surface. These equations are so written that if the radiance is measured for various values of ϕ then a value for the scattering coefficient can be obtained. Following this, equations relating R to ϕ are developed. Finally the relationships between positions on the picture of the horizon and values of ϕ are discussed as well as the relationship of exposure of the film at those positions to apparent radiance of the sea surface.

2.3 In equation 1 which follows, first order scattering theory is used to describe the apparent radiance $N(\phi)$ of the sea surface at angle ϕ below the line to the horizon.

$$N(\phi) = \int_0^R E(r) \Phi(r) \sigma(r) e^{-\int_0^r \sigma(r) dr} e^{-\int_0^R \sigma(r) dr} dr + E(R) g(R) e^{-\int_0^R \sigma(r) dr} \quad (1)$$

where $N(\phi)$ = the apparent radiance of the sea surface at angle ϕ below the line to the horizon.

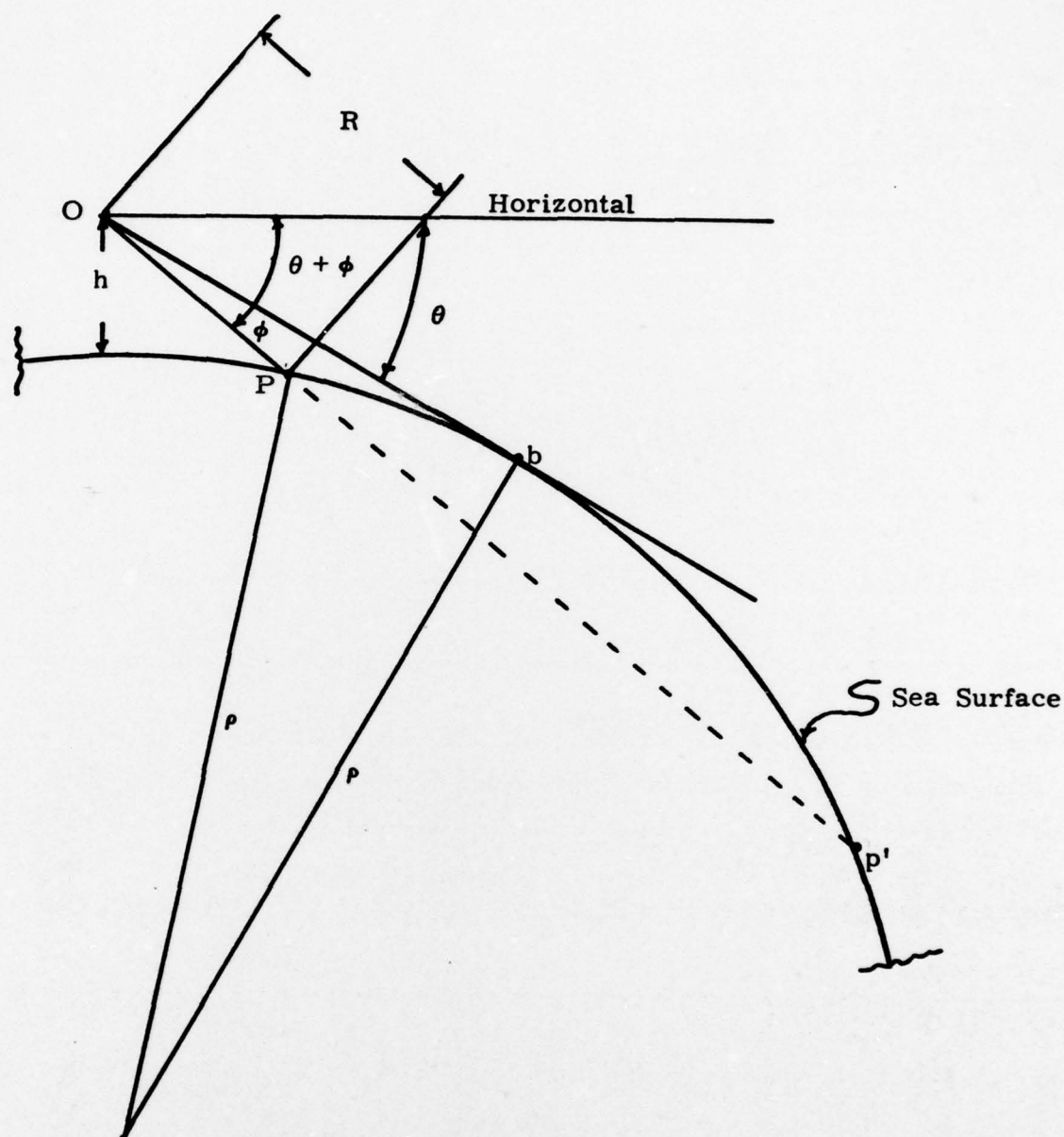


Figure 1. Geometry of the Problem.

Geometry used:

h = height observer's eye in meters

θ = dip of the horizon in minutes

$\theta + \phi$ = dip of point in question in minutes

R = distance to point in kilometers

From Bowditch:

$$R = 2.232 (\theta + \phi) - \sqrt{4.982 (\theta + \phi)^2 - 15.35 h}$$

$$\theta = 1.76 \sqrt{h}$$

$E(r)$ = total irradiance at position r along path
 $\sigma(r)$ = the effective phase function for scattering
 from position r toward observing point.
 $\sigma(r)$ = scattering coefficient at r .
 $g(R)$ = a coefficient such that $g(R) E(R)$ is the
 inherent radiance of the sea surface in the
 direction of the observing point.

2.4 Equation 1 can be solved if three assumptions are made.
 The first is that the irradiance along the path is constant, the second is
 that the phase function along the path is constant, and the third is that
 the inherent radiance of the sea surface is the same for all positions ob-
 served. With these assumptions equation 1 may be written

$$N(\phi) = E \Phi \left[1 - e^{-\int_0^R \sigma(r) dr} \right] + E g e^{-\int_0^R \sigma(r) dr} \quad (2)$$

The derivative of this radiance as a function of the range to the sea
 surface, R , is

$$\frac{d}{dR} N(\phi) = E (\Phi - \rho) \sigma(R) e^{-\int_0^R \sigma(r) dr} \quad (3)$$

When the data has been taken in the presence of fog there is some range
 R^* (corresponding to some value of $\phi = \phi^*$) over which the transmission
 is essentially zero. This implies

$$e^{-\int_0^{R^*} \sigma(r) dr} \longrightarrow 0 \quad R \geq R^* \quad (4)$$

In clear weather the horizon can be seen so there is no path to the sea surface satisfying equation 4. However, the path just above the horizon is assumed to involve sufficient atmosphere that equation 4 holds. For these two cases, represented by ϕ^* which is positive in fog and negative in clear weather, substitution of equation 4 in equation 2 leads to

$$N(\phi^*) = E\phi \quad (5)$$

2.5 The difference between equation 5 and equation 2 is given in equation 6

$$N(\phi^*) - N(\phi) = E(\phi - \rho) e^{-\int_0^R \sigma(r) dr} \quad (6)$$

Finally, equation 3 divided by equation 6 gives the value of the scattering coefficient at distance R. This is shown in equation 7

$$\sigma(R) = \frac{1}{N(\phi^*) - N(\phi)} \frac{d}{dR} N(\phi) \quad (7)$$

This may also be written

$$\begin{aligned} \sigma(R) &= - \frac{1}{N(\phi^*) - N(\phi)} \frac{d}{dR} \{ N(\phi^*) - N(\phi) \} \\ &= - \frac{d}{dR} \ln \{ N(\phi^*) - N(\phi) \} \\ &= - \frac{d}{dR} [\ln \{ N(\phi^*) - N(\phi) \} - \ln N(\phi^*)] \\ &= - \frac{d}{dR} \ln \left\{ \frac{N(\phi^*) - N(\phi)}{N(\phi^*)} \right\} \end{aligned} \quad (8)$$

This is the key equation for the work discussed here. Further discussion of equation 8 and its application to the data reduction will be made easier by an understanding of the relationship of R to ϕ . Equations showing that relationship are developed next.

2.6 Two methods are given here for calculating the distance to a point short of the horizon when the height of the observed is known and the angle of depression of the point relative to the horizon is measured. The first method has its origin in geometrical calculations with no corrections for atmospheric refraction and the second method used empirical relationships which are sensitive to refractive effects and are taken from Bowditch³.

2.7 In Figure 1 an observer at O views at distance R a point p short of the horizon b . The dip angle of the horizon is θ and the dip angle of the point is $\theta + \phi$. The altitude of the observer is h and the radius of the earth is ρ . Using the cosine law one may write

$$\rho^2 + (\rho + h)^2 + R^2 - 2(\rho + h)r \cos(\pi/2 - (\theta + \phi))$$

$$\text{or } R^2 - 2(\rho + h)r \sin(\theta + \phi) + 2\rho h + h^2 = 0 \quad (9)$$

Solving for R gives

$$R = (\rho + h) \sin(\theta + \phi) \pm \sqrt{(\rho + h)^2 \sin^2(\theta + \phi) - 2\rho h - h^2} \quad (10)$$

The solution with the positive radical is appropriate to point p' in Figure 1. The solution with the negative radical is appropriate for this development as it relates to the point p which is short of the horizon. When the radical is equal to zero the points p and p' are coincident and the line of

sight is directed to the horizon. In this case

$$\sqrt{(\rho + h)^2 \sin^2 (\theta + \phi) - 2 \rho h - h^2} = 0$$

$$\text{or } \sin^2 \theta = \frac{2 \rho h - h^2}{(\rho + h)^2}$$

$$\text{and } \theta = \sin^{-1} \sqrt{\frac{2 \rho h - h^2}{(\rho + h)^2}} \quad (11)$$

This is the dip of horizon assuming no refraction. Now equation 10 may be written

$$R = (\rho + h) \sin (\theta + \phi) \sqrt{1 - \frac{\sin^2 \theta}{\sin^2 (\theta + \phi)}} \quad (12)$$

Equations 11 and 12 make up the geometrical solution for the relationship between R and ϕ .

2.8 Bowditch gives an expression for the dip of a point short of the horizon which is rewritten here in metric units as

$$(\theta + \phi) = 0.224R + 3.440 h/R \quad (13)$$

where

$(\theta + \phi)$ is the dip of the point in minutes

h is the height of the observers eye in minutes

and R is the distance to the point in kilometers.

Solving equation 13 for R, the distance to the point short of the horizon gives

$$R = 2.232 (\theta + \phi) - \sqrt{4.982 (\theta + \phi)^2 - 15.35 h} \quad (14)$$

For the case $\phi = 0$ (the line to the horizon)

$$\sqrt{4.982\theta^2 - 15.35h} = 0$$

or $\theta = 1.76 \sqrt{h}$ (15)

2.9 For the 1977 EOMET work the value of h , the height of the camera lens above the sea surface, was 4.60 meters. Using the geometrical equations gives θ , the depression of the horizon, as 4.13 minutes and the distance to the horizon as 7.656 km. Using Bowditch's equations gives θ as 3.775 min. and the distance to the horizon as 7.810 km. In Figure 2 the range to the horizon calculated using Bowditch's equation, R_{Bowd} , is shown as a function of ϕ . The figure also shows the ratio δ where

$$\delta = \frac{R_{\text{Bowd}} - R_{\text{Geom}}}{R_{\text{Bowd}}} \quad (16)$$

In the data reduction done here Bowditch's equations are used.

2.10 Equation 8 relates $\sigma(R)$, the scattering coefficient at range R , to the observable radiances $N(\phi^*)$ and $N(\phi)$ where $N(\phi^*)$ is the radiance just above the horizon or, in fog, at a dip angle ϕ^* small enough so that the specular transmission to the sea surface approaches zero. Equation 8 is repeated here

$$\sigma(R) = -\frac{d}{dR} \ln \left\{ \frac{N(\phi^*) - N(\phi)}{N(\phi^*)} \right\} \quad (8)$$

Equation 14 is the expression from Bowditch for R , km, the range to a point short of the horizon, when the point has a dip $(\theta + \phi)$, min. the

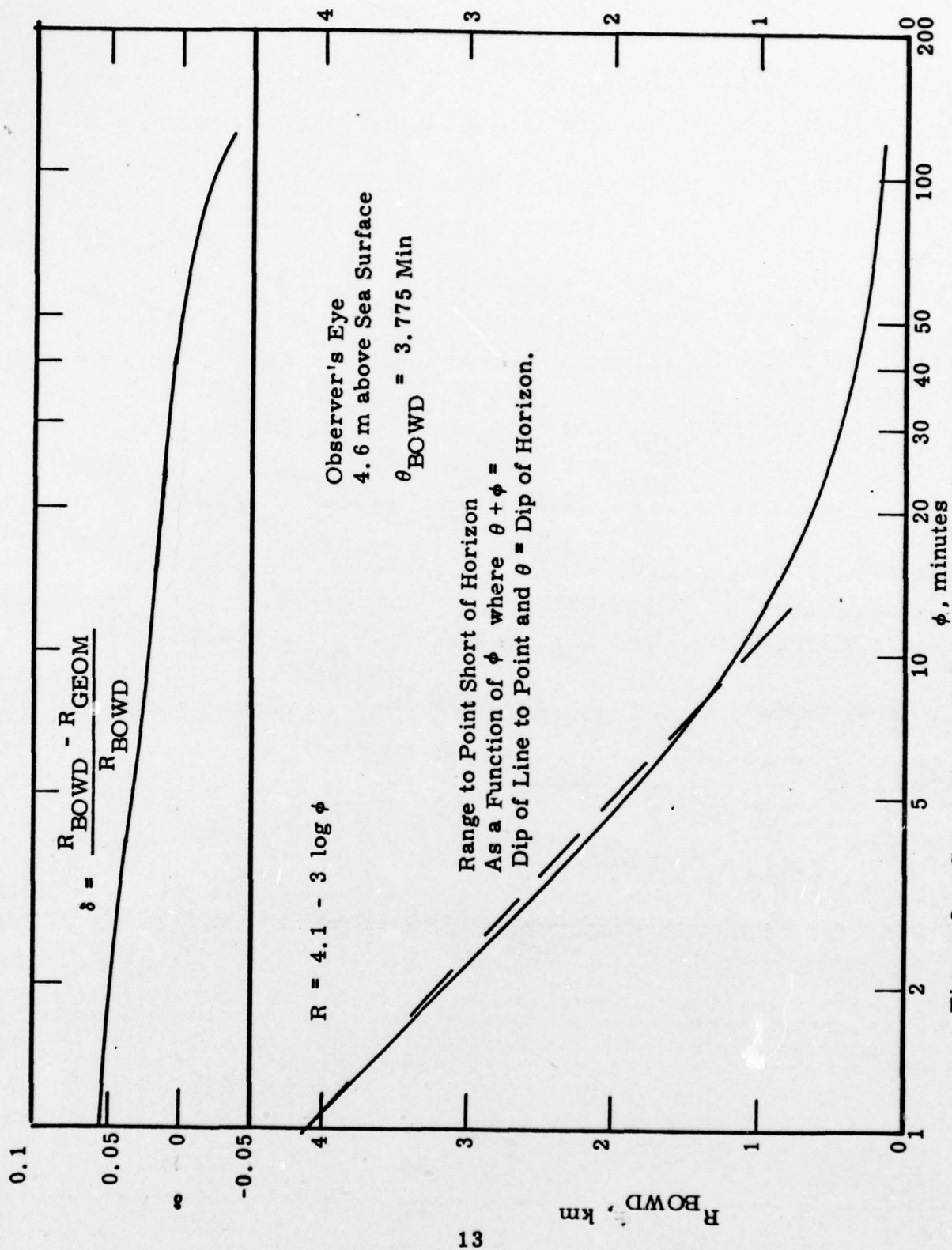


Figure 2. Comparison of Geometric Solution to Bowditch.

horizon has a dip θ , min and the observer is a height h , m, above the sea surface. As shown in Figure 2, when $h = 4.6$ m the relationship of R to ϕ in the range $1 \leq \phi \leq 10$ min can be given by the approximate expressions

$$R = 4.1 + 3 \log \phi \quad (16a)$$

$$\text{and} \quad \frac{dR}{d\phi} = - \frac{1.3}{\phi} \quad (16b)$$

$$\text{so} \quad \frac{1}{R} \frac{dR}{d\phi} = \frac{-1.3}{\phi (4.1 - 3 \log \phi)} \quad (16c)$$

2.11 In the EOMET experiments h was 4.6 m and the lens of the camera used had a focal length of 50mm. The resolution of the film used was, at best, 50 lines per mm. In a rough way the angular resolution may be taken as $\Delta \alpha = \tan^{-1} \frac{0.02}{50} = 1.38$ min. The probable error in assigning location of the horizon is of the class of \pm one resolution element, or ± 1.38 min. Table 1 presents calculations using equation 16c of ΔR the uncertainty in range R to points short of the horizon due to $\pm \Delta \alpha$, the uncertainties in the location of the horizon. One film resolution element is taken as the value of $\Delta \alpha$. Values of ΔR are calculated for true distances on the film below the horizon from one to ten resolution elements in length.

2.12 In the EOMET experiments there was no effort made to hold the camera exactly horizontal or to point it exactly at the horizon. Location of the horizon image on the films introduces uncertainties in angular position of points short of the horizon of the order of ± 1.375 min. This uncertainty makes the determination of scattering coefficient as a function of

TABLE 1. ERROR ANALYSIS

Number of film resolution elements from horizon	ϕ , min	R, km	$\Delta R = \frac{dR}{d\phi} \Delta \alpha$	$\frac{\Delta R}{R}$
0	0	7.810		
1	1.375	3.685	± 1.3	$+ 0.35$
2	2.750	2.782	± 0.65	± 0.23
3	4.125	2.254	± 0.43	± 0.19
4	5.500	1.879	± 0.33	± 0.17
5	6.875	1.588	± 0.26	± 0.16
6	8.250	1.351	± 0.22	± 0.16
7	9.625	1.150	± 0.19	± 0.16

In this table ΔR is the uncertainty in range R to point short of horizon. True point position, ϕ , in minutes, is associated with the number of resolution elements on film below the horizon image. The uncertainty in locating the horizon is $\pm \Delta \alpha$ where $\Delta \alpha$ is taken to be equal to one resolution element which for the lens and film used is 1.375 min.

range, $\sigma(R)$, by use of equation 8 essentially impossible. In a fall-back position it is assumed that the scattering coefficient $\sigma(R) = \sigma$; that is, that the scattering coefficient is independent of range then, from equation 8

$$-\frac{d}{dR} \sigma(R) = 0 = \frac{d^2}{dR^2} \ln \left\{ \frac{N(\phi^*) - N(\phi)}{N(\phi^*)} \right\} \quad (17)$$

and

$$-\frac{d}{dR} \ln \left\{ \frac{N(\phi^*) - N(\phi)}{N(\phi^*)} \right\} = \text{const} = \sigma \quad (18)$$

or a plot of

$$-\ln \left\{ \frac{N(\phi^*) - N(\phi)}{N(\phi^*)} \right\} \text{ vs } R$$

must be a straight line with slope equal to σ

2.13 Figure 3 presents plots of the function

$$f(\phi) = \ln \left\{ \frac{N(\phi^*) - N(\phi)}{N(\phi^*)} \right\} \quad (19)$$

vs

$$R(\phi + \Delta\phi)$$

where ϕ is the correct value of the angle between the line to the point in question and the line to the horizon and $\Delta\phi$ is the error in that value.

Curve A has no error and is a straight line as required by equation 18.

Curves B have errors of ± 0.34 min (corresponding to 0.25 pixels on film)

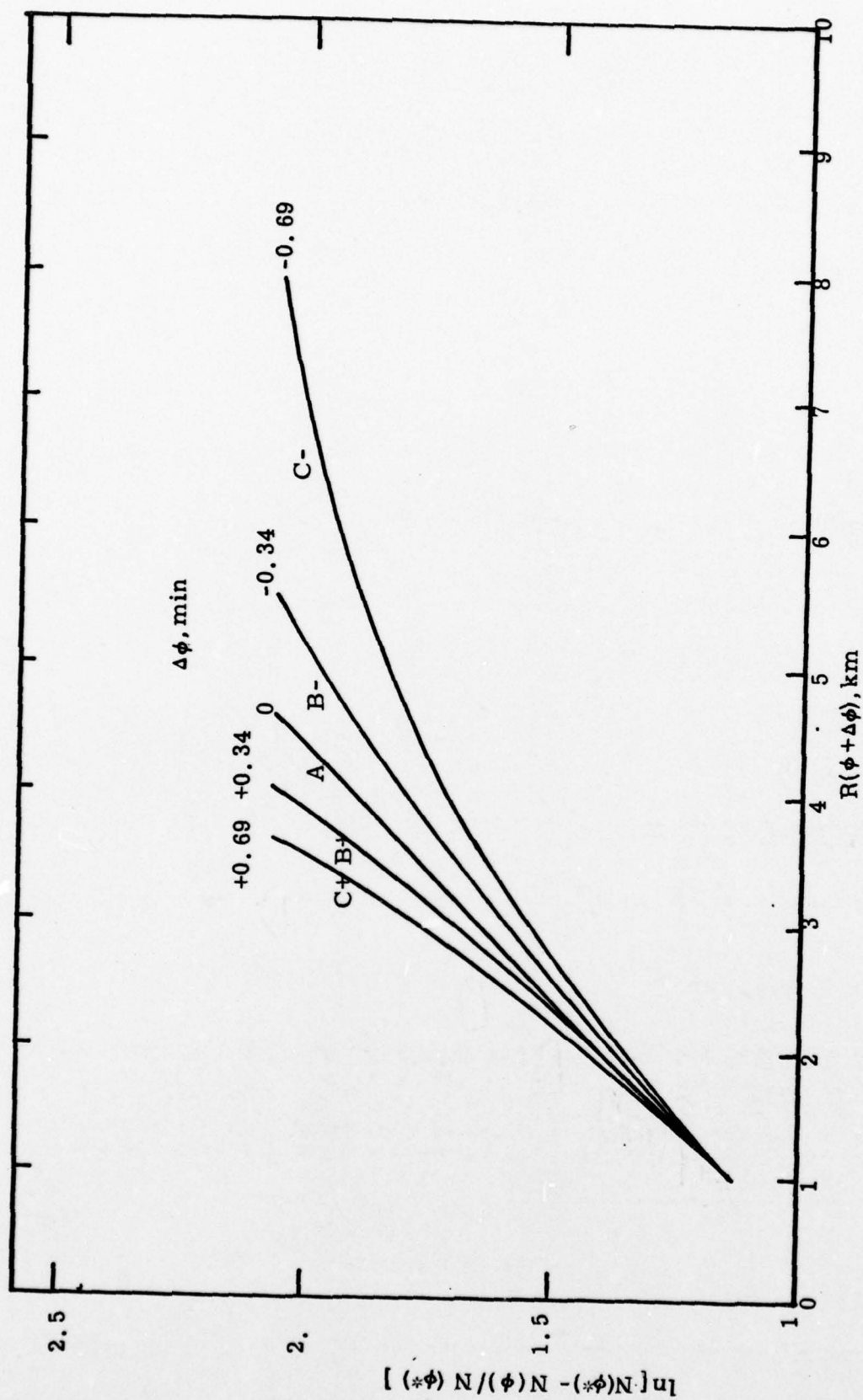


Figure 3. Effects of error in assumed position of horizon.

and curves C have errors of ± 0.69 min. In this illustration the range to the horizon is 7.97 km and the correct value of R for point 1 is 4.62 km. There is nothing unique about this. The positive or negative curvature of the plot which results from incorrect guess of horizon image position is characteristic of any case of $R < 7.97$ km. This feature will be discussed again when the techniques of data reduction are described.

3. DATA REDUCTION

3.1 Ektachrome-X film was used for the EOMET horizon photographs. All of the film had the same emulsion number and it was all processed by Eastman Kodak in a single batch along with appropriate sensitometric exposures. Ektachrome-X is a positive color film and by using appropriate optical filters in data reduction the film response in three wavelength bands can be determined. These bands center on wavelengths 0.44μ , 0.55μ , and 0.64μ . A Photometrics Data Systems Microdensitometer was used in data reduction and the first step of the process was to use the sensitometric exposures to establish at each of the three wavelengths the relationship between film density and relative exposure.

3.2 Figure 4 is a sketch showing the path on the processed horizon photographs scanned by the microdensitometer. The densitometer slit, which was 1300μ long and 17μ wide was set parallel to the horizon and moved from a position one millimeter above the best guess of horizon image location to a position 5 mm below that location. The density of the film was read automatically every 20μ along the track and these readings were recorded on tape. This process was carried out for each of the three colors, blue, green, and red which were selected by incorporating in the optical train of the densitometer Wratten filters No. 94, No. 93, and No. 92 respectively.

3.3 A simple program was set up for a CDC 6600 computer which used the sensitometer data to convert density to relative exposure for each of the three colors. The product of this program is a properly annotated print out of the step number and relative exposure associated with the microdensitometer track across the horizon image. Figure 5 is such a print out and is for frame 13 of the film exposed on 24 May 1977 at 1355. This microdensitometer run was made using a Wratten Filter No. 94, which is blue. The best guess of horizon position was assigned

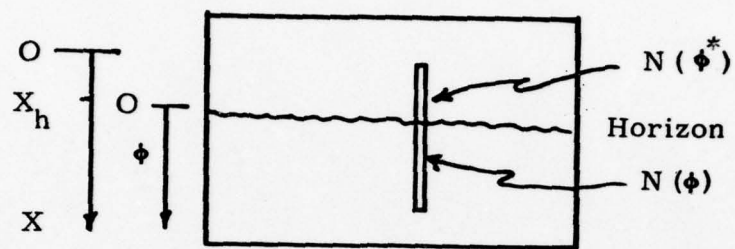


Figure 4. Scanning Track of Photographs

FOMET VISIBILITY DATA REDUCTION PROGRAM
RELATIVE EXPOSURE VS POSITION (MM)

FILM SEGMENT FRAME DATE TIME IDEN COLOR
8 5 13 24 MAY 7 1355 P3508NPS01 BLUE 94

TW

X (MM)	REL EXP	X (MM)	REL EXP	X (MM)	REL EXP	X (MM)	REL EXP	X (MM)	REL EXP
9.00	11.16	9.02	11.16	9.04	11.16	9.06	11.33	9.08	11.00
9.10	11.16	9.12	11.16	9.14	11.16	9.16	11.16	9.18	11.00
9.20	11.16	9.22	11.00	9.24	11.16	9.26	11.16	9.28	11.16
9.30	11.00	9.32	11.00	9.34	10.84	9.36	10.84	9.38	10.84
9.40	10.84	9.42	10.84	9.44	10.84	9.46	11.00	9.48	11.00
9.50	11.00	9.52	10.84	9.54	10.84	9.56	10.84	9.58	10.84
9.60	10.84	9.62	10.84	9.64	11.00	9.66	10.84	9.68	10.84
9.70	10.84	9.72	10.84	9.74	11.00	9.76	10.84	9.78	11.00
9.80	10.84	9.82	11.00	9.84	10.84	9.86	11.00	9.88	10.84
9.90	10.84	9.92	11.00	9.94	10.84	9.96	11.00	9.98	10.84
10.00	10.68	10.02	10.37	10.04	8.68	10.06	7.53	10.08	7.15
10.10	6.79	10.12	6.79	10.14	6.61	10.16	6.61	10.18	6.35
10.20	6.19	10.22	6.03	10.24	6.19	10.26	6.03	10.28	6.03
10.30	5.95	10.32	6.03	10.34	5.95	10.36	5.95	10.38	5.87
10.40	5.72	10.42	5.80	10.44	5.80	10.46	5.95	10.48	5.87
10.50	5.72	10.52	5.65	10.54	5.65	10.56	5.57	10.58	5.57
10.60	5.45	10.62	5.45	10.64	5.50	10.66	5.45	10.68	5.35
10.70	5.40	10.72	5.35	10.74	5.40	10.76	5.35	10.78	5.45
10.80	5.35	10.82	5.35	10.84	5.30	10.86	5.21	10.88	5.35
10.90	5.30	10.92	5.21	10.94	5.16	10.96	5.25	10.98	5.30
11.00	5.40	11.02	5.35	11.04	5.35	11.06	5.30	11.08	5.21
11.10	5.25	11.12	5.35	11.14	5.21	11.16	5.16	11.18	5.30
11.20	5.11	11.22	5.16	11.24	5.40	11.26	5.35	11.28	5.21
11.30	5.25	11.32	5.21	11.34	5.87	11.36	5.25	11.38	5.45
11.40	5.45	11.42	5.45	11.44	5.40	11.46	5.30	11.48	5.16
11.50	5.21	11.52	5.16	11.54	4.97	11.56	4.97	11.58	5.16
11.60	5.25	11.62	5.40	11.64	5.35	11.66	5.50	11.68	5.21
11.70	5.25	11.72	5.16	11.74	5.07	11.76	4.88	11.78	4.71
11.80	4.84	11.82	4.84	11.84	4.75	11.86	5.02	11.88	5.21
11.90	5.40	11.92	5.57	11.94	5.65	11.96	5.45	11.98	5.40
12.00	5.45	12.02	5.35	12.04	5.35	12.06	5.25	12.08	5.30
12.10	5.50	12.12	5.35	12.14	5.02	12.16	4.84	12.18	4.62
12.20	4.54	12.22	4.88	12.24	5.11	12.26	5.16	12.28	5.30
12.30	5.16	12.32	4.84	12.34	4.75	12.36	4.88	12.38	4.97
12.40	5.07	12.42	4.93	12.44	4.67	12.46	4.80	12.48	4.88
12.50	4.93	12.52	4.97	12.54	4.93	12.56	4.62	12.58	4.58
12.60	4.38	12.62	4.38	12.64	4.42	12.66	4.42	12.68	4.67
12.70	5.07	12.72	5.25	12.74	5.40	12.76	5.35	12.78	5.16
12.80	5.15	12.82	5.40	12.84	5.02	12.86	4.50	12.88	4.42
12.90	4.50	12.92	4.88	12.94	4.93	12.96	4.80	12.98	5.11
13.00	5.45	13.02	5.35	13.04	5.16	13.06	5.02	13.08	5.07
13.10	5.16	13.12	5.30	13.14	5.25	13.16	4.97	13.18	5.07
13.20	5.25	13.22	5.30	13.24	5.07	13.26	5.07	13.28	5.07
13.30	5.02	13.32	4.97	13.34	4.88	13.36	4.80	13.38	4.75
13.40	4.93	13.42	4.97	13.44	5.02	13.46	4.97	13.48	5.07
13.50	5.07	13.52	5.11	13.54	5.16	13.56	5.21	13.58	5.25
13.60	5.16	13.62	5.11	13.64	4.97	13.66	5.07	13.68	5.11
13.70	5.07	13.72	5.16	13.74	5.21	13.76	5.16	13.78	5.11
13.80	5.07	13.82	4.71	13.84	4.42	13.86	4.34	13.88	4.50
13.90	4.54	13.92	4.88	13.94	5.11	13.96	5.11	13.98	5.25
14.00	5.21	14.02	4.88	14.04	4.38	14.06	4.38	14.08	4.71
14.10	5.02	14.12	5.07	14.14	4.84	14.16	4.54	14.18	4.75
14.20	4.93	14.22	5.02	14.24	5.25	14.26	5.25	14.28	4.88
14.30	4.71	14.32	4.33	14.34	4.38	14.36	4.67	14.38	4.97
14.40	5.11	14.42	4.71	14.44	4.34	14.46	4.54	14.48	4.67
14.50	4.75	14.52	4.97	14.54	5.02	14.56	5.02	14.58	5.21
14.60	5.07	14.62	4.93	14.64	4.88	14.66	4.71	14.68	4.67
14.70	4.54	14.72	4.42	14.74	4.22	14.76	4.14	14.78	4.34
14.80	4.50	14.82	4.75	14.84	4.80	14.86	4.67	14.88	4.54
14.90	4.88	14.92	5.07	14.94	4.88	14.96	4.84	14.98	4.75
15.00	4.62								

10.89

Figure 5. Values of relative exposure from horizon trace.

track distance scale value of 10.00 mm. The trace was started above the horizon image at 9.00 mm and run to 15.00 mm.

3.4 The relative exposure values for the 15 points between 9.60 mm and 10.84 mm were averaged (10.89) and used as $N(\phi^*)$ the relative radiance of the sky above the horizon. The exposures in the sequence starting at 9.98 were scanned visually and sequential differences noted. The exposure (8.68 at 10.04) following the greatest sequential difference (10.37-8.68) was selected as the first of a series of nine values of $N(\phi)$ to be used in calculating the scattering coefficient.

3.5 A program for an HP-97 was used to calculate

$$f(x - x_0) = -\ln \left\{ \frac{N(\phi^*) - N(\phi)}{N(\phi^*)} \right\} \quad (20)$$

for each of the nine values of $N(\phi)$ and also the ranges, R , for each of the nine values of $(x - x_0)$ in the microdensitometer track assuming some position x_0 for the horizon. The HP-97 program calculated the linear regression corresponding to

$$f(x - x_0) = A + BR(x - x_0) \quad (21)$$

for the first five values of $(x - x_0)$, yielding B_5 and then for the nine values of $(x - x_0)$, yielding B_9 . The ratio B_5/B_9 was calculated and if this was within one percent of unity the selected position for the horizon was accepted otherwise a new position for the horizon (x_0) was chosen. Usually no more than four such iterations of this sort were necessary. The final value of B_9 , the slope of the regression, was taken as σ , the scattering coefficient. The program then could print out the nine pairs of values $N(\phi)$ and R appropriate to the nine values of $(x - x_0)$. The following values

from Figure 4 were used in this process:

$N(\phi^*)$	=	10.89	
$N(\phi), 1$	=	8.68	at 10.04
2	=	7.53	10.06
3	=	7.15	10.08
4	=	6.78	10.10
5	=	6.78	10.12
6	=	6.61	10.14
7	=	6.61	10.16
8	=	6.35	10.18
9	=	6.19	10.20

In the iteration to find the horizon position the following values of x_o were used resulting in the associated values of B_5/B_9 .

x_o	B_5/B_9
10.03	1.18
10.04	0.975
10.375	1.06
10.039	1.02
10.0395	1.008

Using the value $x_0 = 10.0395$ values of $f(x-x_0)$ and R are

R, km	$f(x-x_0)$
7.18	1.59
3.62	1.18
2.65	1.07
2.12	0.974
1.77	0.974
1.53	0.934
1.35	0.934
1.20	0.850
1.09	0.840

The regression is given by

$$f(x-x_0) = 0.744 + 0.119 R (x-x_0) \quad (22)$$

hence $\sigma = 0.119 \approx 0.12 \text{ km}^{-1}$.

3.6 In this work 30 films have been analyzed in three colors leading to 90 possible values of σ . Of these 53 have been done as described above, 12 have been done using nine averages of sequential groups of five (45 values of $N(\phi)$ in total), 3 have been done with sequential groups of fifteen and one with sequential groups of 3. Of the remaining 21, 18 have been done by hand and involved less than five groups of from 1 to 15 values of $N(\phi)$ per group and three defied analysis. Values of σ so obtained are presented in Table 2.

TABLE 2. Values of Scattering Coefficient, km^{-1}

Date	Time	Demonstration			Challenge		
		0.44μ	0.55μ	0.64μ	0.44μ	0.55μ	0.64μ
May 17	1320	2.42	1.95	1.63 (5, 9)			
	18 0945	<u>28</u>	<u>8.5</u>	<u>3.5</u> (15, 6)	<u>3.48</u>	3.17	2.79 (15, 9)
	18 1700	0.12	0.11	0.10 (1, 9)	0.20	0.15	0.08 (1, 9)
	21 1545	0.21	0.17	0.10 (1, 9)	<u>0.36</u>	<u>0.24</u>	<u>0.28</u> (1, 5)
	22 1230	0.19	0.22	0.20 (1, 9)	<u>0.62</u>	<u>0.52</u>	<u>0.51</u> (1, 5)
	22 1830	0.08	0.06	0.08 (1, 9)	0.23	0.29	0.29 (1, 9)
	23 1100	0.16	0.13	0.12 (1, 9)			
	24 1030	0.25	0.18	0.19 (1, 9)			
	24 1355	0.12	0.08	0.06 (1, 9)	1.45	1.25	1.29 (5, 9)
	25 1055	0.17	0.19	0.17 (1, 9)			
	25 1610	0.13	0.085	0.086 (1, 9)			
	26 0925	0.27	0.33	0.21 (1, 9)	<u>0.51</u>	<u>0.42</u>	<u>0.45</u> (1, 5)
	26 1530	0.43	0.31	0.25 (1, 9)	<u>0.41</u>	<u>0.36</u>	<u>0.47</u> (1, 4)
	27 0950	4.09	2.97	1.99 (5, 9)			
	31 1050	0.37	0.29	0.19 (1, 9)	Failure		
June	1 1240	0.16	0.14	0.12 (1, 9)			
	3 1230	0.16	0.15	0.19 (1, 9)			
	4 1505	0.56	0.45	0.35 (1, 9)			
	5 1440	0.67	0.53	0.38 (1, 9)	<u>1.61</u>	<u>0.92</u>	<u>1.08</u> (5, 4)
	6 1330	0.92	0.91	0.85 (5, 9)			

DEMONSTRATION VALUES ARE FROM FRAME SELECTED VISUALLY AS EASIEST TO REDUCE.

CHALLENGE VALUES ARE FROM FRAMES SELECTED VISUALLY TO BE PROPERLY EXPOSED BUT DIFFICULT TO REDUCE.

UNDERLINED VALUES OBTAINED BY SPECIAL HAND PROCESSING.

OTHER VALUES OBTAINED BY SEMI-HANDS-OFF METHOD.

VALUES IN PARENTHESES (1, 9), (15, 6) etc REPRESENT NUMBER OF SEQUENTIAL VALUES OF $N(\phi)$ AVERAGED IN A GROUP FOLLOWED BY NUMBER OF GROUPS INVOLVED IN A PLOT.

3.7 Each value of σ quoted in Table 2 represents the slope of an associated plot of values of $f(x - x_0)$ vs $R(x - x_0)$. All such plots are presented in Appendix A. The processed data from each horizon photograph analyzed (with the exception of the one failure) is presented in the appendix as three plots drawn on one page. These are the plots of

$$\ln \left\{ \frac{N(\phi^*) - N(\phi)}{N(\phi^*)} \right\} = f(x - x_0) \text{ vs } R(x - x_0).$$

The plots are for the blue, the green and the red image of the horizon. The plots are identified by date and Greenwich mean time. The letter D in the upper right hand corner identifies a demonstration run and the letter C a challenge. The values of total scattering coefficient, which is the slope of the plots shown, are given for the three colors as are the associated aerosol scattering coefficients. Certain meteorological information with the plots and other supporting information is given in Table 3.

TABLE 3. PHYSICAL AND METEOROLOGICAL CONDITIONS

MONTH	DAY	GMT	Latitude	Longitude	True Wind Direct.	Ship Head. True	% Cloud Cover
			deg. min.	deg. min.	deg.	deg.	
May	17	1320	42 37.889	65 32.402	229	043	20 Ac Trans
	18	0945	44 37.043	62 4.712	318	060	Fog-xx
	18	1700	45 9.000	60 32.8	136	061	<1 Ci Fibr.
	21	1545	44 50.1	42 2.0	318	099	100 xx
	22	1230	44 16.1	37 4.4	300	274	40 Cu Fair Weather
	22	1830	44 5.1	36 58.45	290	097	90 Cu Fair Weather, Ci Fibr.
	23	1100	43 30.7	31 37.7	020	105	50 Sc Cumulog, Ac Trans undul, Ci Fibr.
	24	1030	43 6.159	25 30.027	178	100	100 xx Rain
	24	1355	41 58.4	24 37.0	175	100	100 xx
	25	1055	40 34.6	19 23.0	187	114	60 Ac Trans overhead downto 30°
	25	1610	40 8.1	18 14.8	198	113	100 St cover Rainclouds 3000 ft.
	26	0925	38 35.25	14 29.95	205	231	100 Cu Fair Weather, Cs
	26	1550	38 30.7	13 50.8	274	115	1 Cs
	27	0950	37 6.0	9 29.45	348	021	20 Fair Weather St, Sc Cumulog
June	31	1050	35 39.0	3 27.9	304	075	80 St Fract, Fair Weather Cu
	1	1240	37 52.9	1 47.9	251	058	100 Ac Trans, As Opacus
	3	1230	36 48.0	-12 23.2	330	145	40 Ci Fibr, Ac Trans, Cu Fair Weather, Sc Cumulog
	4	1505	33 39.1	-15 26.0	311	145	5 Fair Weather Cu
	5	1440	33 7.1	-19 19.0	306	320	50 Fair Weather Cu, Congestus
	6	1330	35 20.7	-22 56.2	310	046	5 Fair Weather Cumulus

4. DISCUSSION

4.1 The demonstration pictures for 19 of the 20 occasions when the horizon was photographed give reasonable values for the total scattering coefficient in the blue the green and the red. These values have been obtained by an almost automatic process of data reduction. Operator involvement occurs in the selection of the best guess position of the horizon and the changes of this guessed position in the iteration process. The twentieth occasion, May 18 at 0945, required hand reduction of the data and yielded unreasonable results. It should be noted that the challenge picture selected for this occasion yielded rather reasonable values of the scattering coefficients.

4.2 The photographs selected as challenges seem to produce reasonable values of the scattering coefficients; however, there is only rather general agreement between simultaneous challenge and the demonstration values. The values on May 24 at 1355 are different by more than an order of magnitude. In this case the demonstration, data reduction was carried out the "automatic" process and involved the use of nine adjacent pixels for data processing. In this case the values of scattering coefficient have been determined by optical effects occurring within the range between approximately 1 and 4.6 km from the ship. The corresponding challenge data were also reduced "automatically" however, using the first nine pixels below the horizon did not work well in the "automatic" process so nine sequential groups of 5 pixels per group were used. In this case the values of scattering coefficient have been determined by optical effects occurring within the approximate range 0.25 to 2.4 km. Inspection of the picture used for the challenge shows a dark streak on the sea extending from about 0.16 km from the ship to roughly 1.3 km. This may account for the results obtained with this film.

4.3 As noted before, the challenge picture for 31 May at 1050 could not be analyzed either "automatically" or by hand.

5. CONCLUSIONS

The following conclusions seem justified:

1. Color photographs of the sea horizon can be used to determine scattering coefficients at $\lambda = 0.44\mu$, $\lambda = 0.55\mu$, $\lambda = 0.64\mu$.
2. The semi-hands-off calculations demonstrate that completely automatic data analysis is feasible.
3. Such an analysis system could be used in a real time system involving, for instance, scanning or a silicon diode array.
4. The existing films could be used as a data bank for simulations of the behavior of proposed real time systems.

REFERENCES

1. H. S. Stewart and A. H. Pierson, J. Opt Soc Am. 64, 550A (1974).
2. Kabanov, M. V. and Sakerin, S. M., "Determination of the Extinction Coefficients for Optical Radiation in the Atmosphere from the Softening of the Horizon Line", Izvestiya, Atmospheric and Ocean Physics, Vol 13, No. 5, 1977.
3. Bowditch, N., "American Practical Navigator", H.O. Pub. No. 9, U.S. Navy Hydrographic Office, 1958.

APPENDIX A

Processed Data

In the following pages three graphs are presented for each film analyzed. Each page is specific to a particular film identified by date and time. In addition the letter D or C identifies demonstration pictures or challenge pictures.

The graphs are of the function

$$\ln \left\{ \frac{N(\phi^*) - N(\phi)}{N(\phi^*)} \right\}$$

vs $R(\phi)$. It has been shown that if the graph is a straight line the locus of the horizon ($\phi = 0$) has been selected correctly and the slope of the straight line is equal to the scattering coefficient.

Twenty pages of graphs representing the reduced data for the demonstration films are presented in sequence of times the pictures were taken.

Following this nine pages of challenge graph are given. Interspersed are five black and white enlargements of the color pictures used. The demonstration picture included is for 3 June at 1230. Challenge pictures are 18 May at 0945, 21 May at 1545, 22 May at 1230 and 22 May at 1830. Finally a print of the densitometer trace across the horizon is given for the blue image on the challenge film for 21 May at 1545.

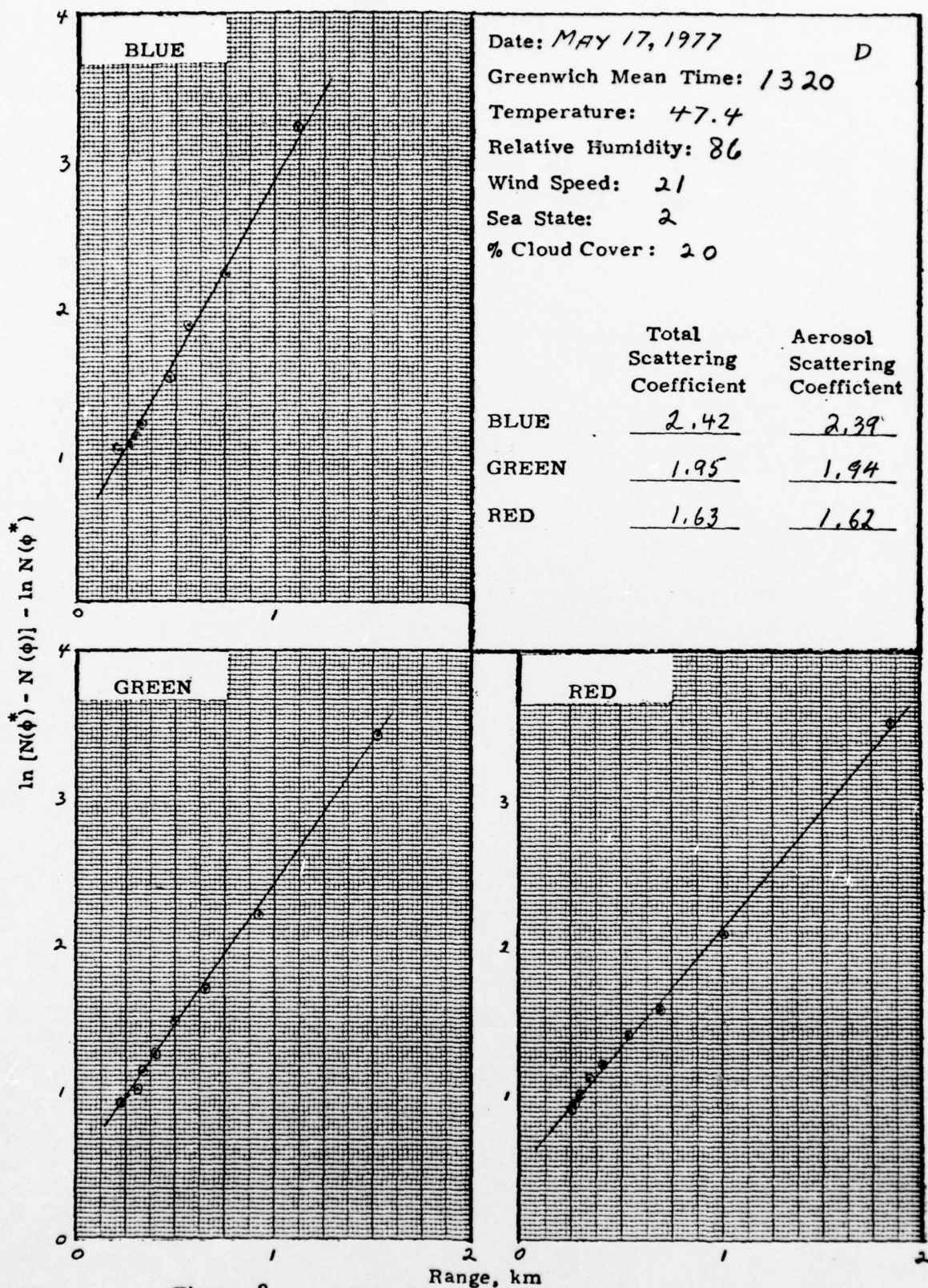


Figure 6.

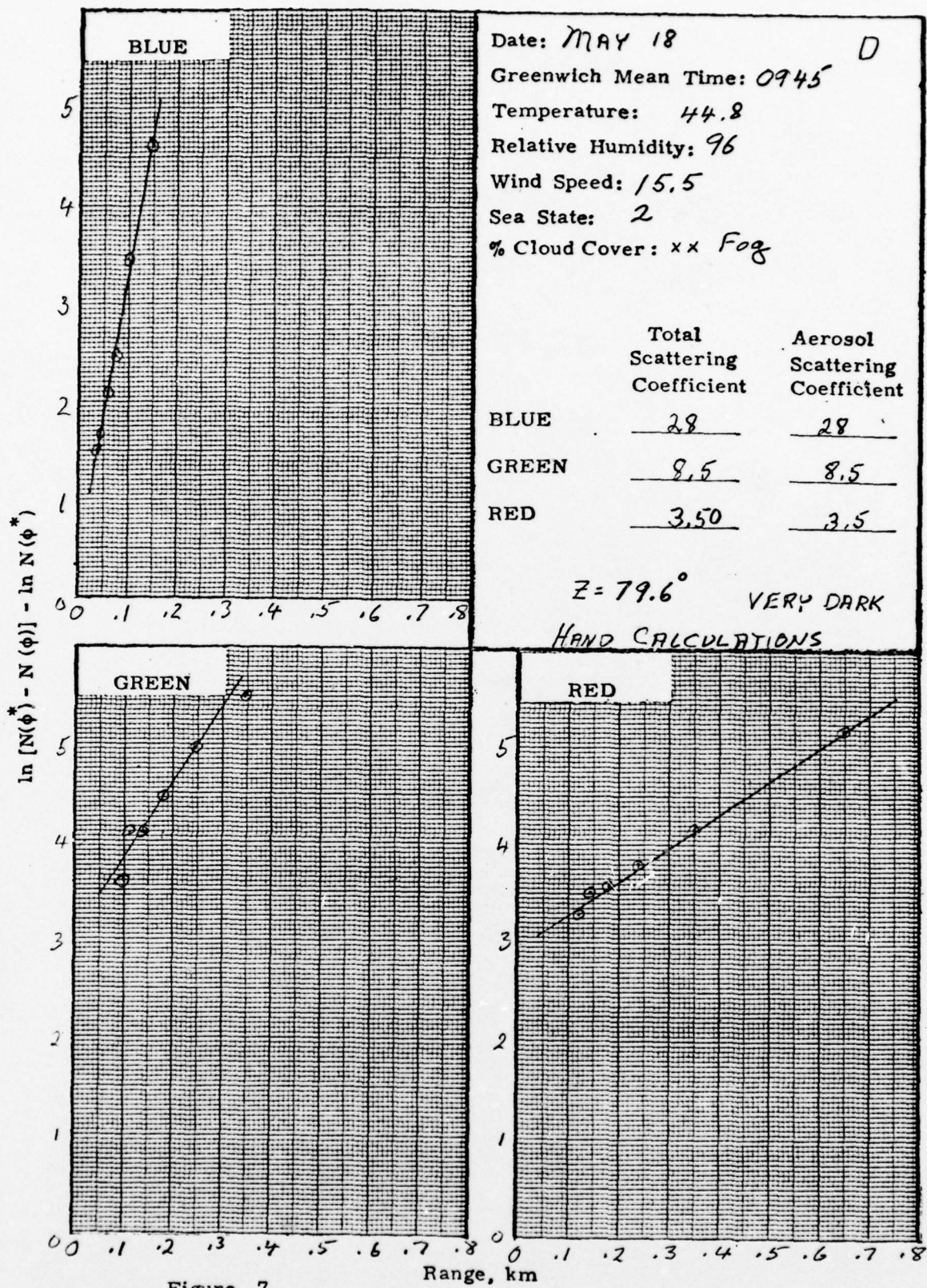


Figure 7

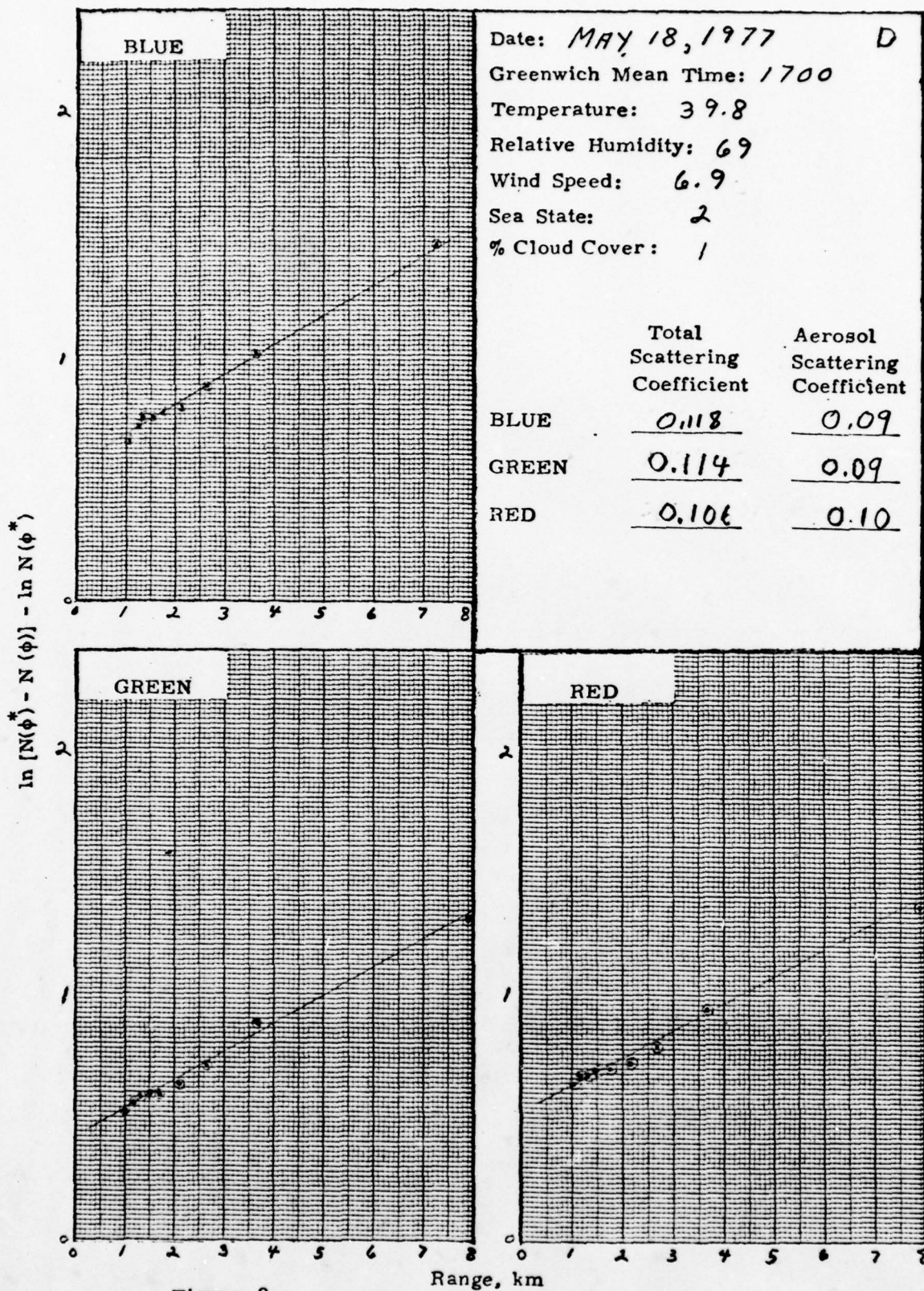


Figure 8.

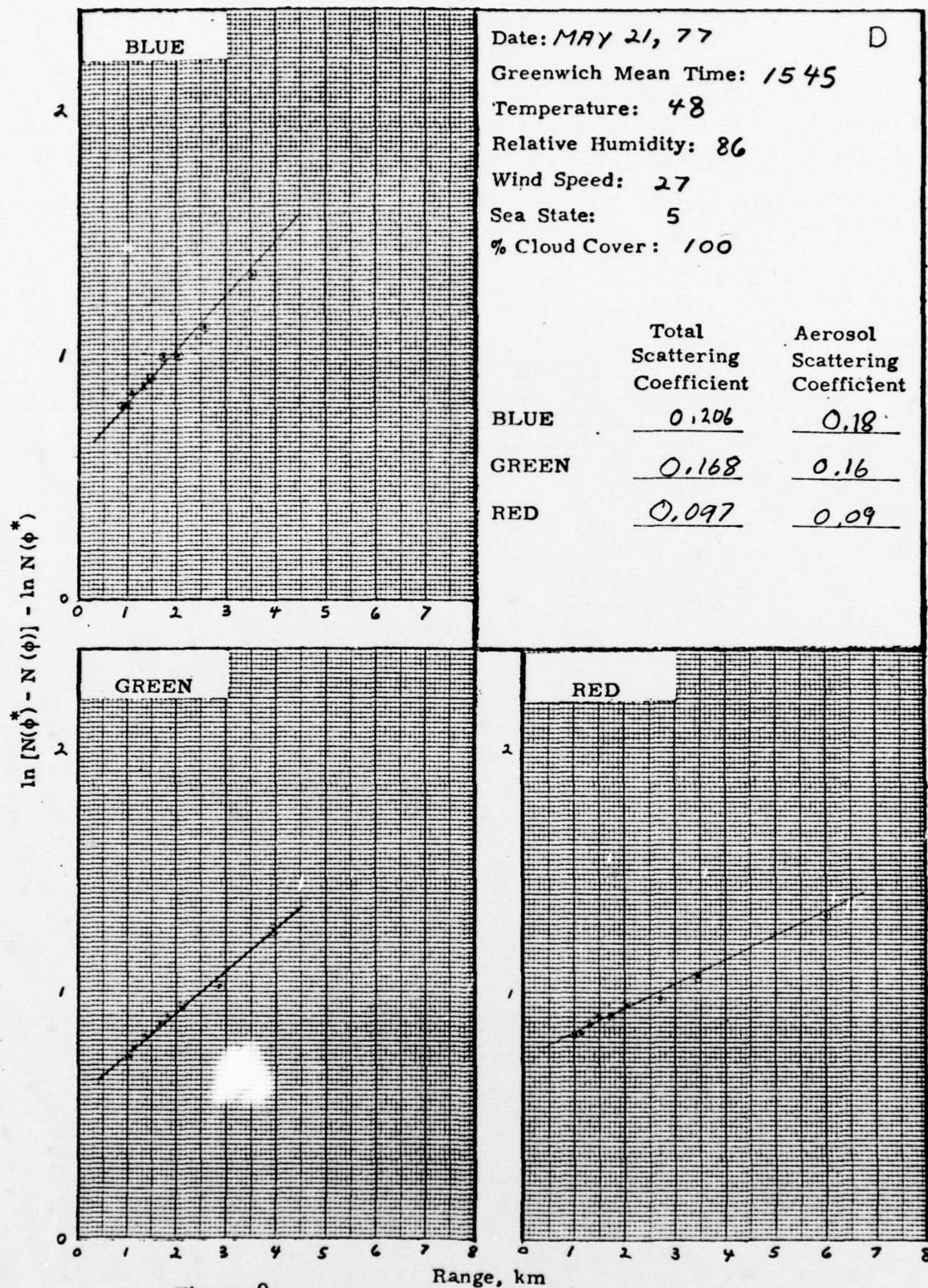


Figure 9

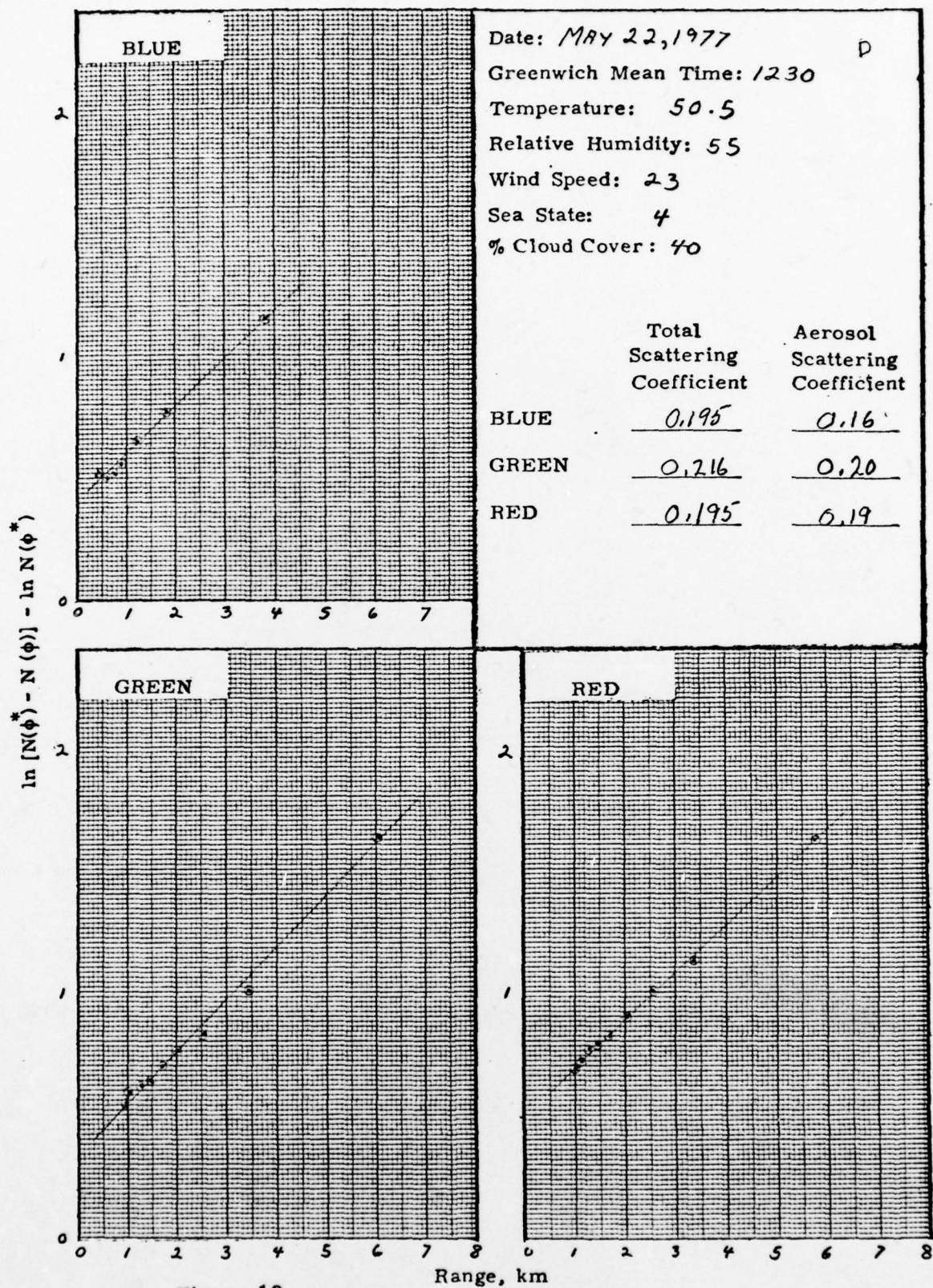
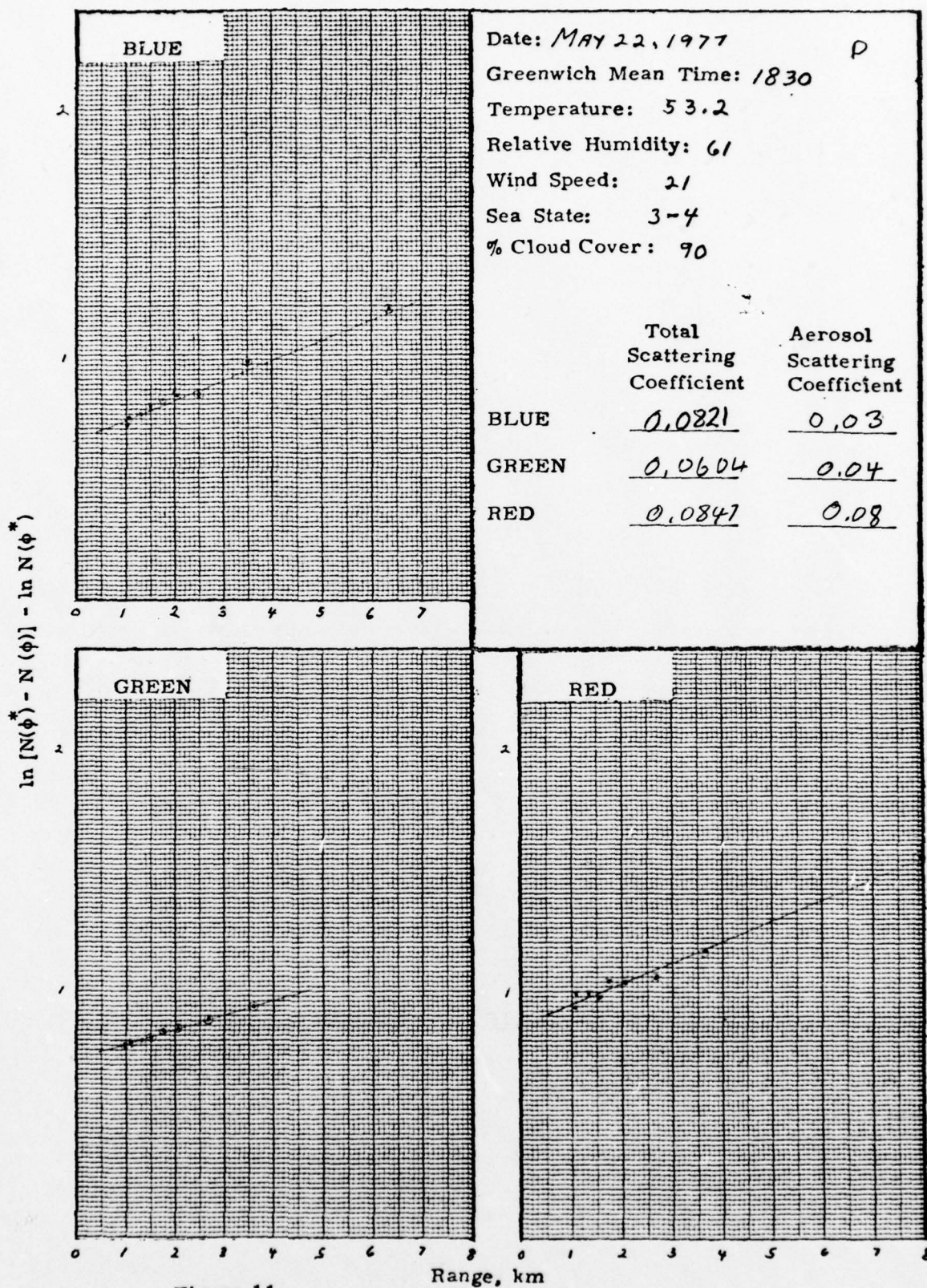


Figure 10



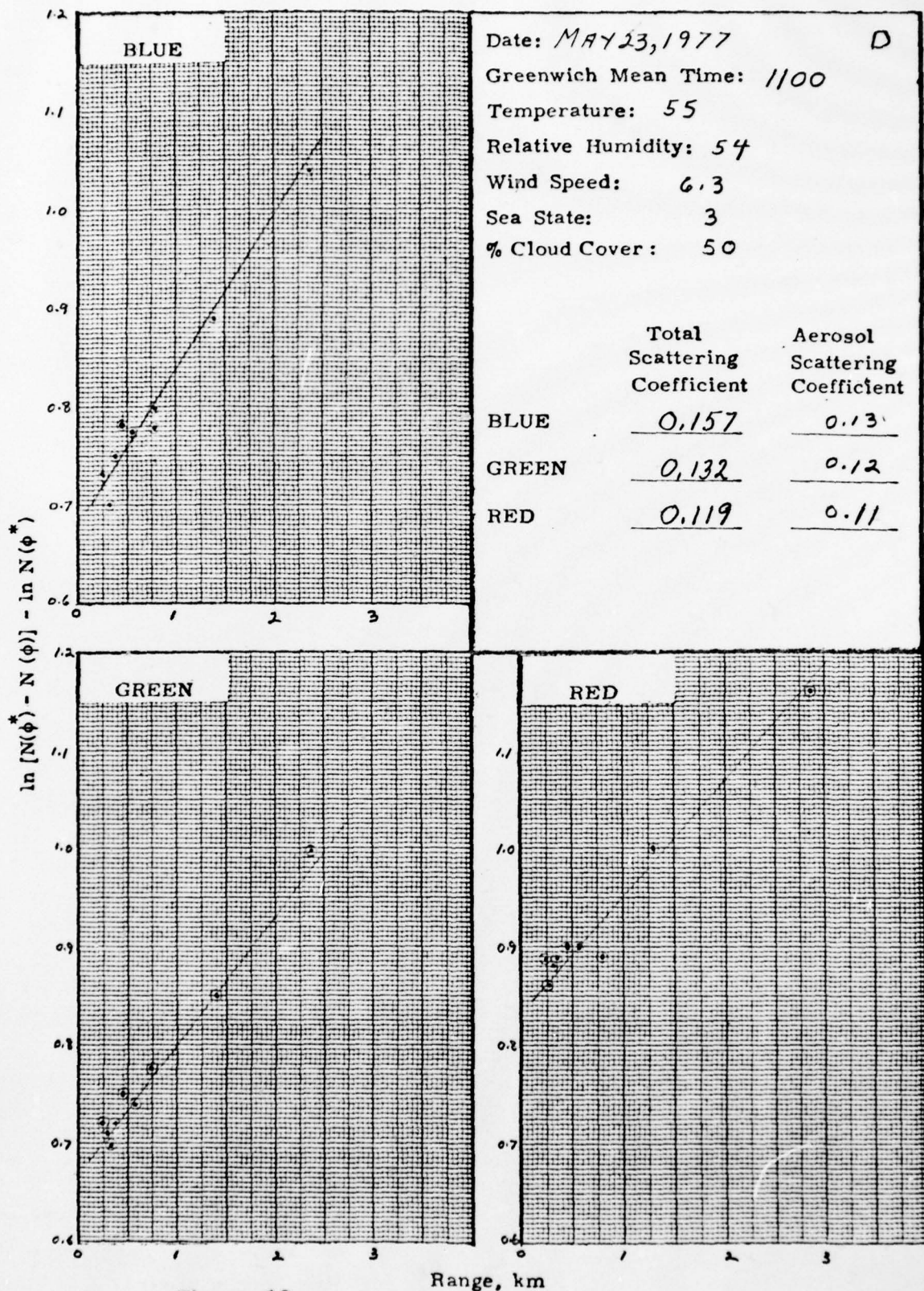
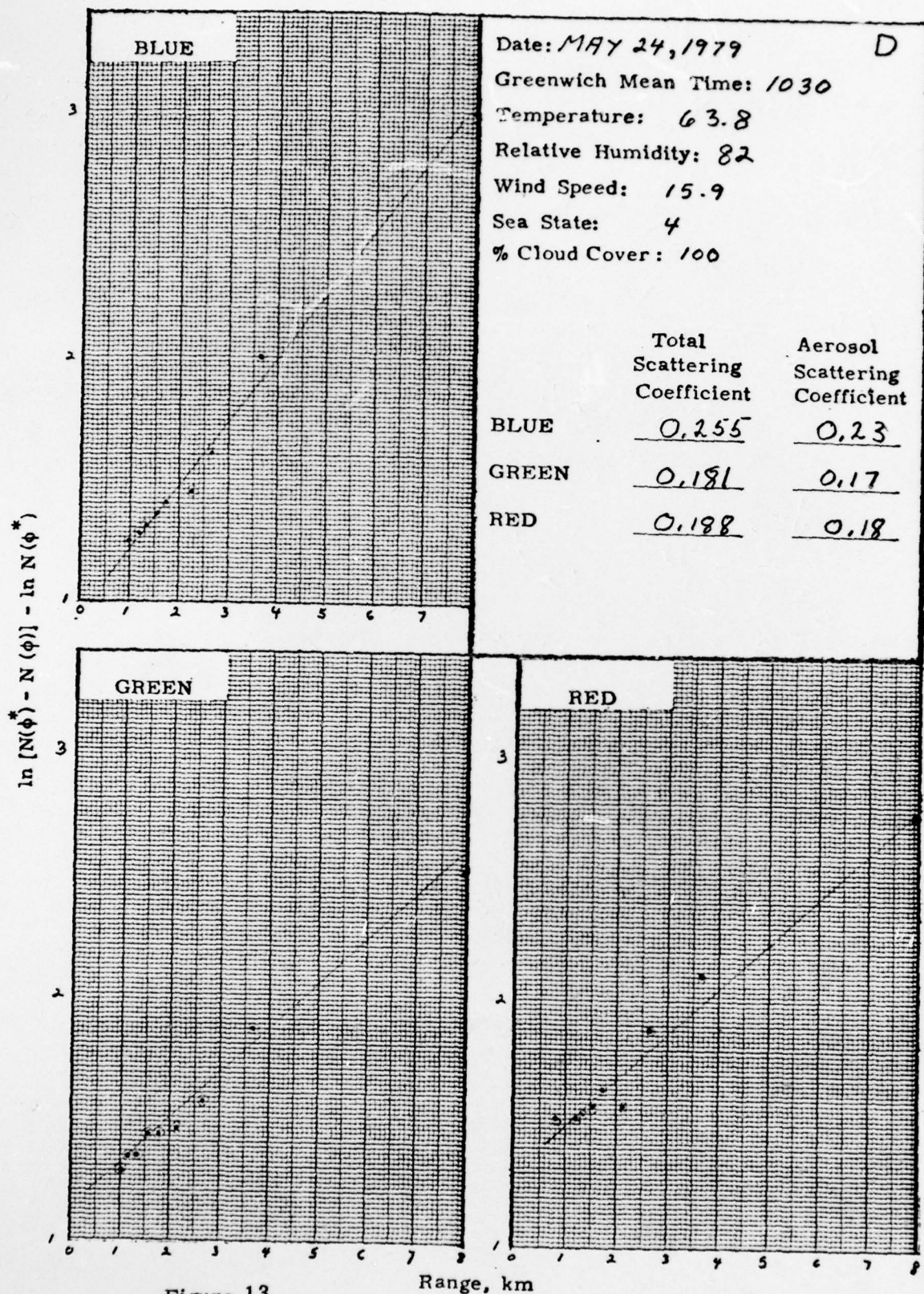


Figure 12



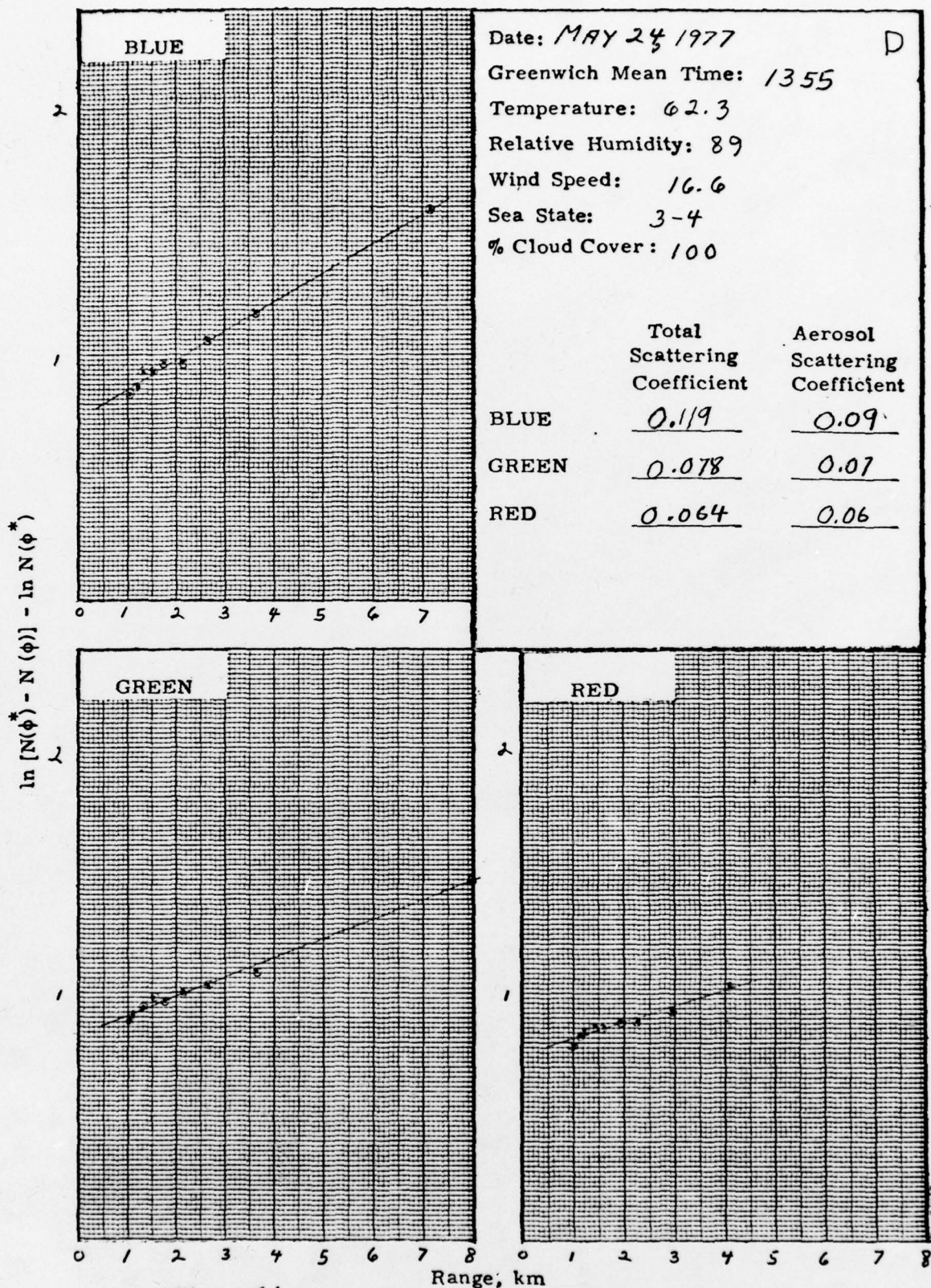


Figure 14

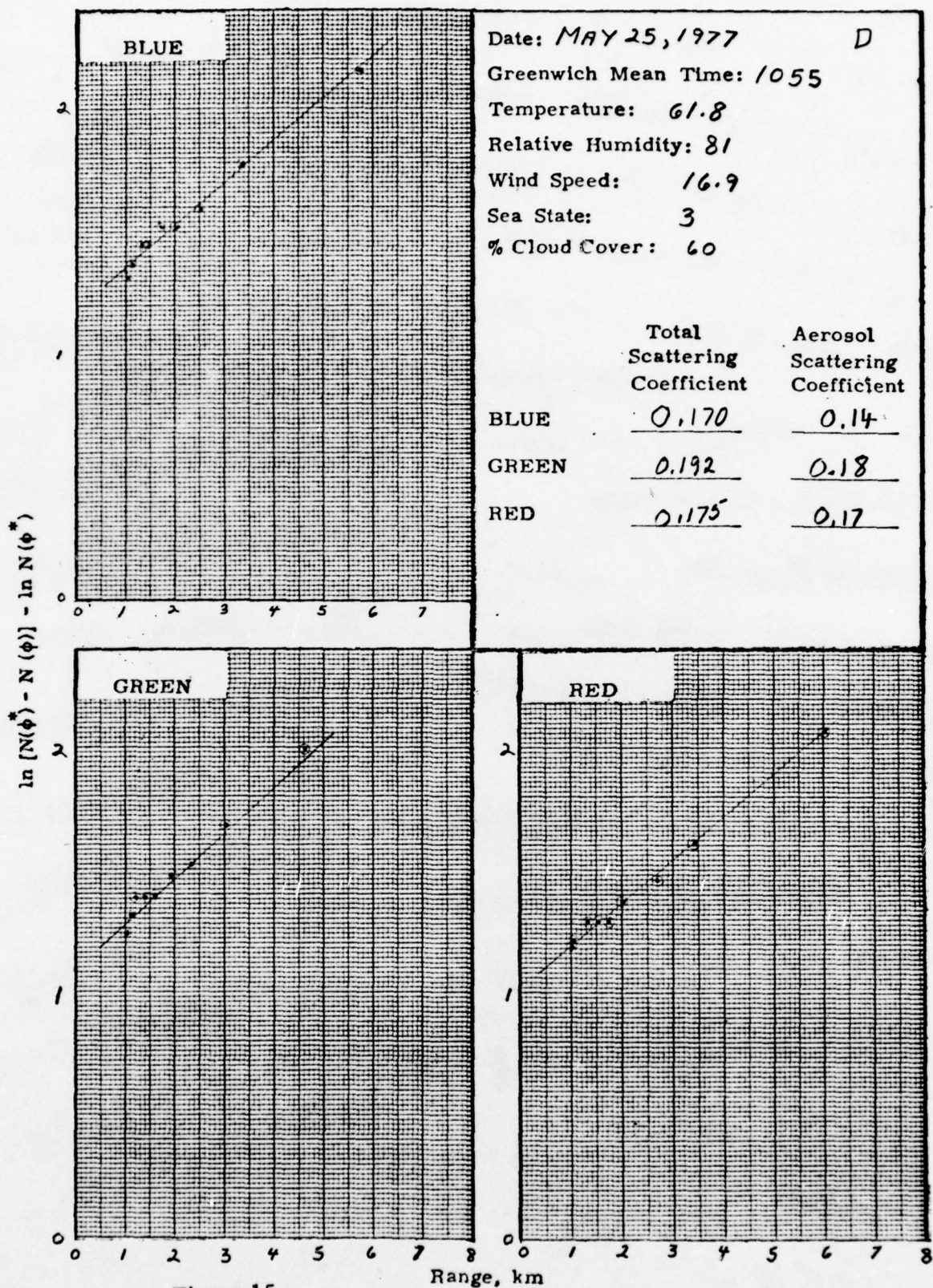


Figure 15

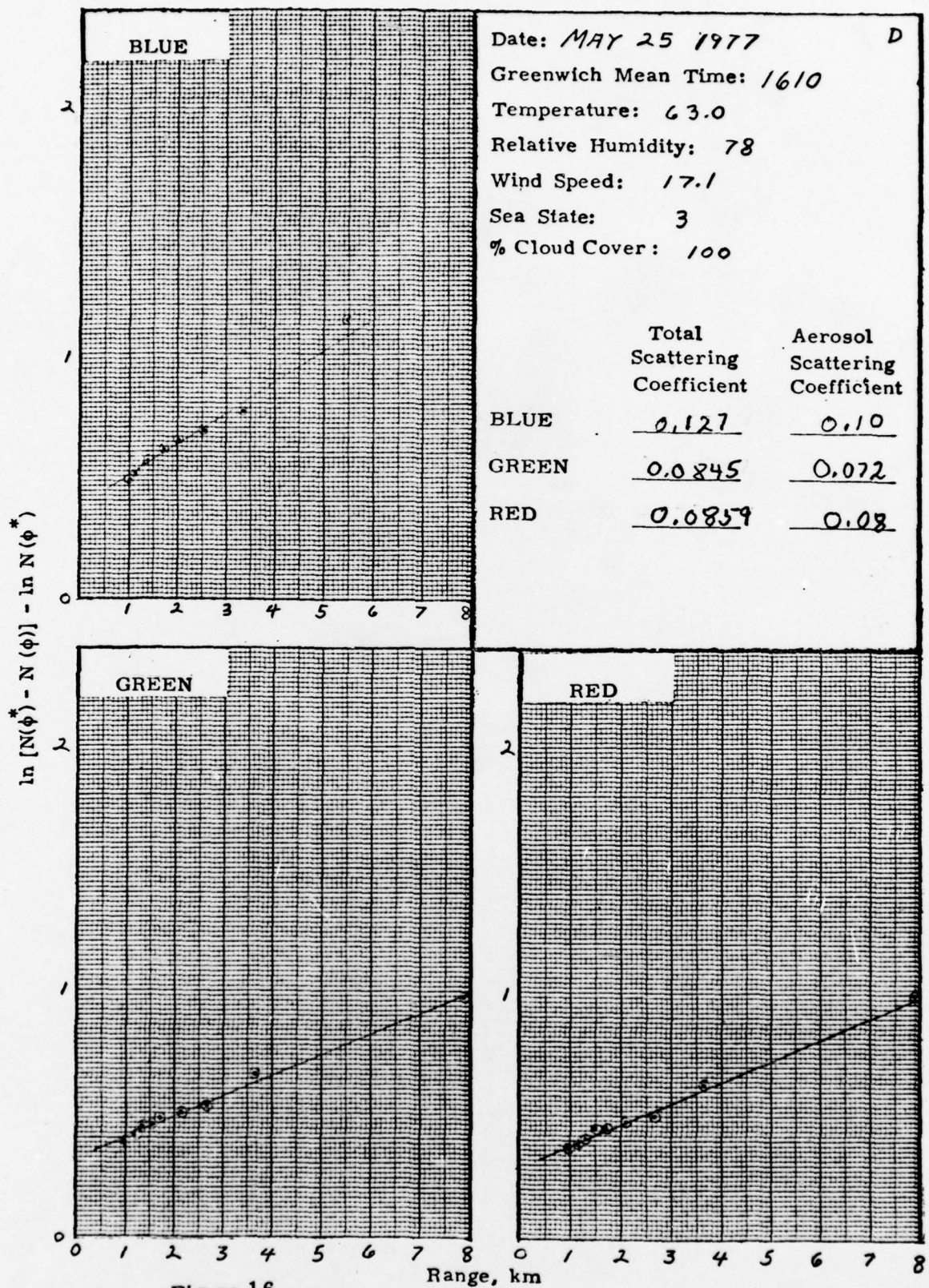


Figure 16

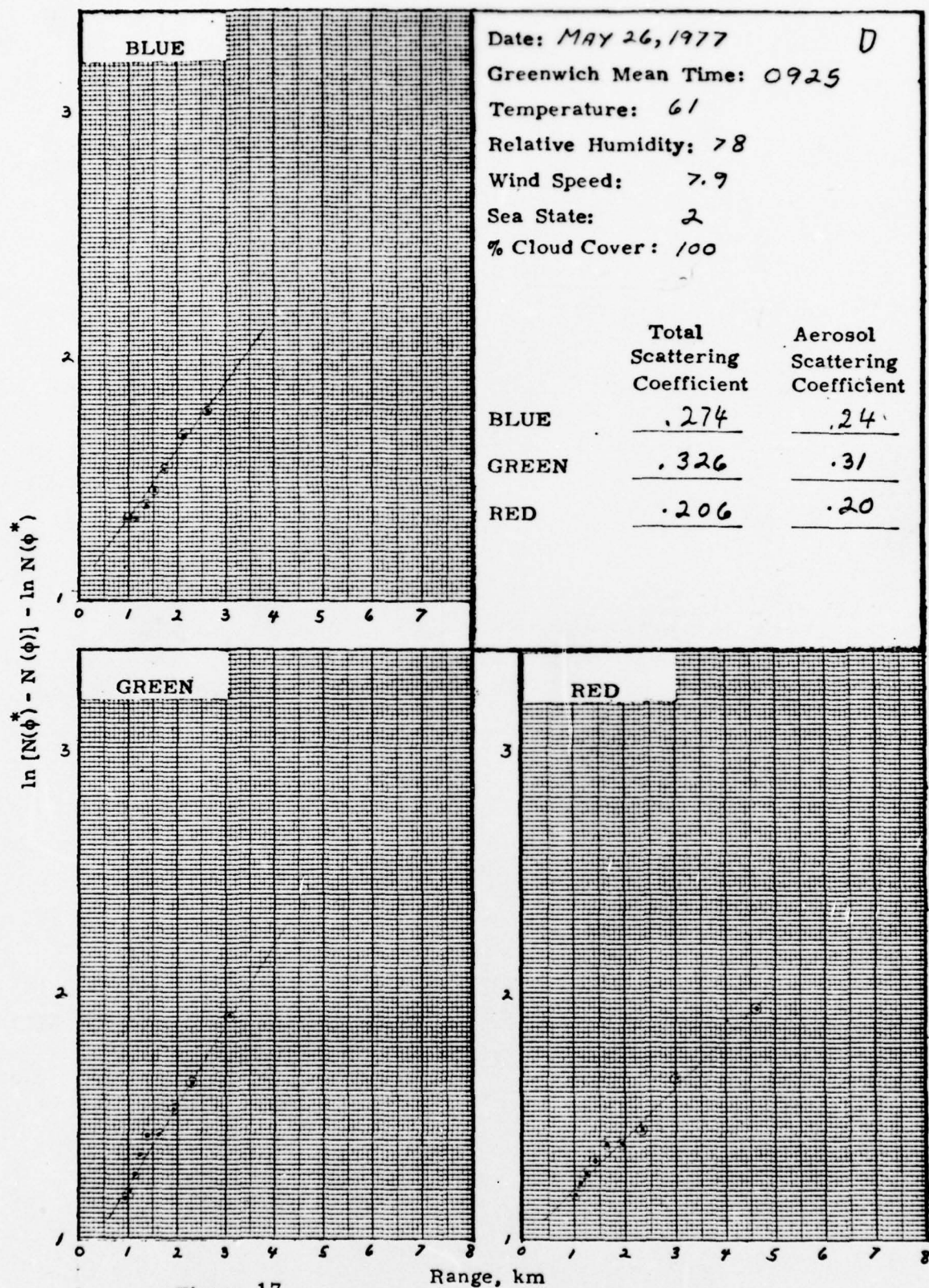


Figure 17

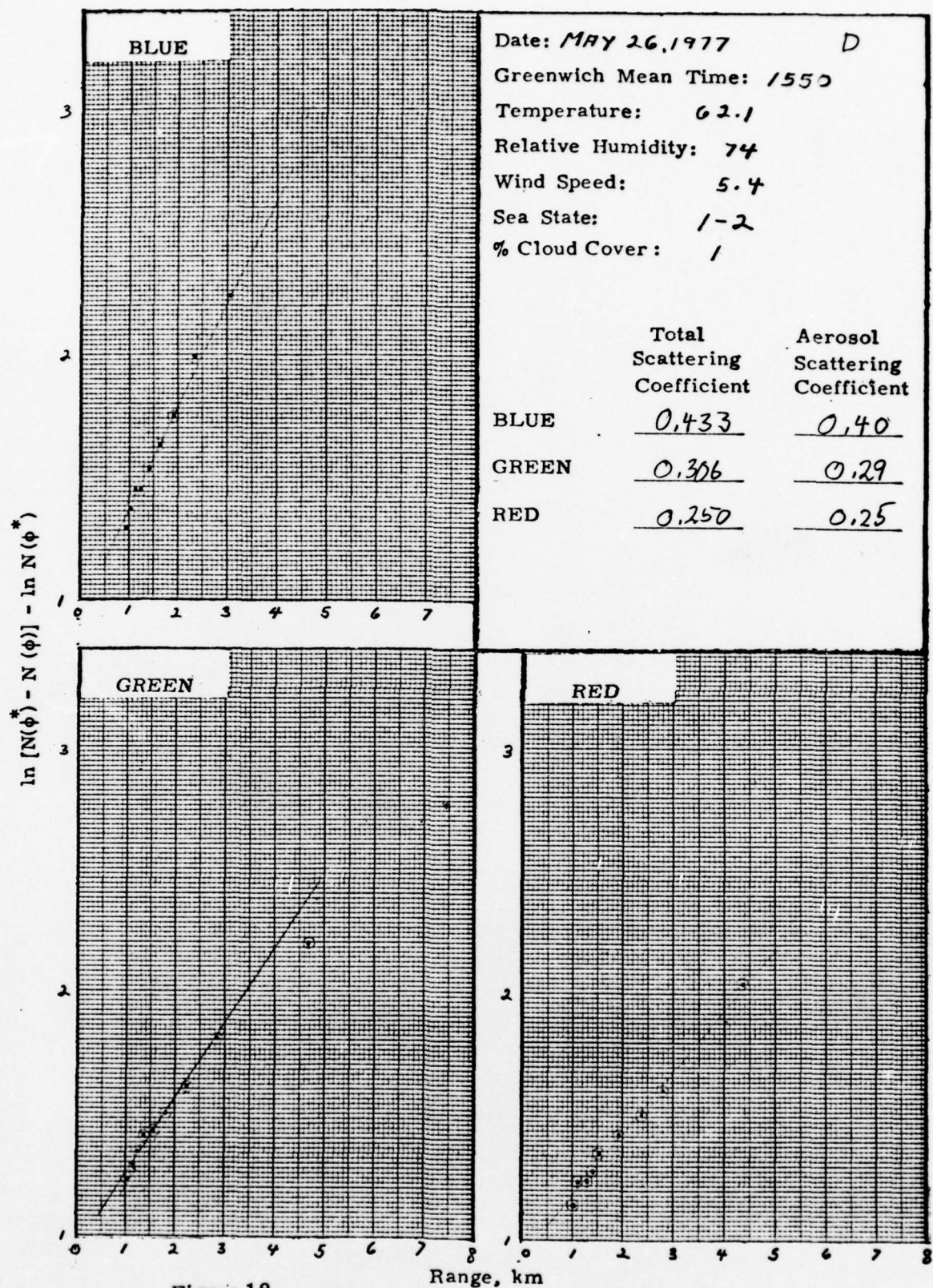


Figure 18

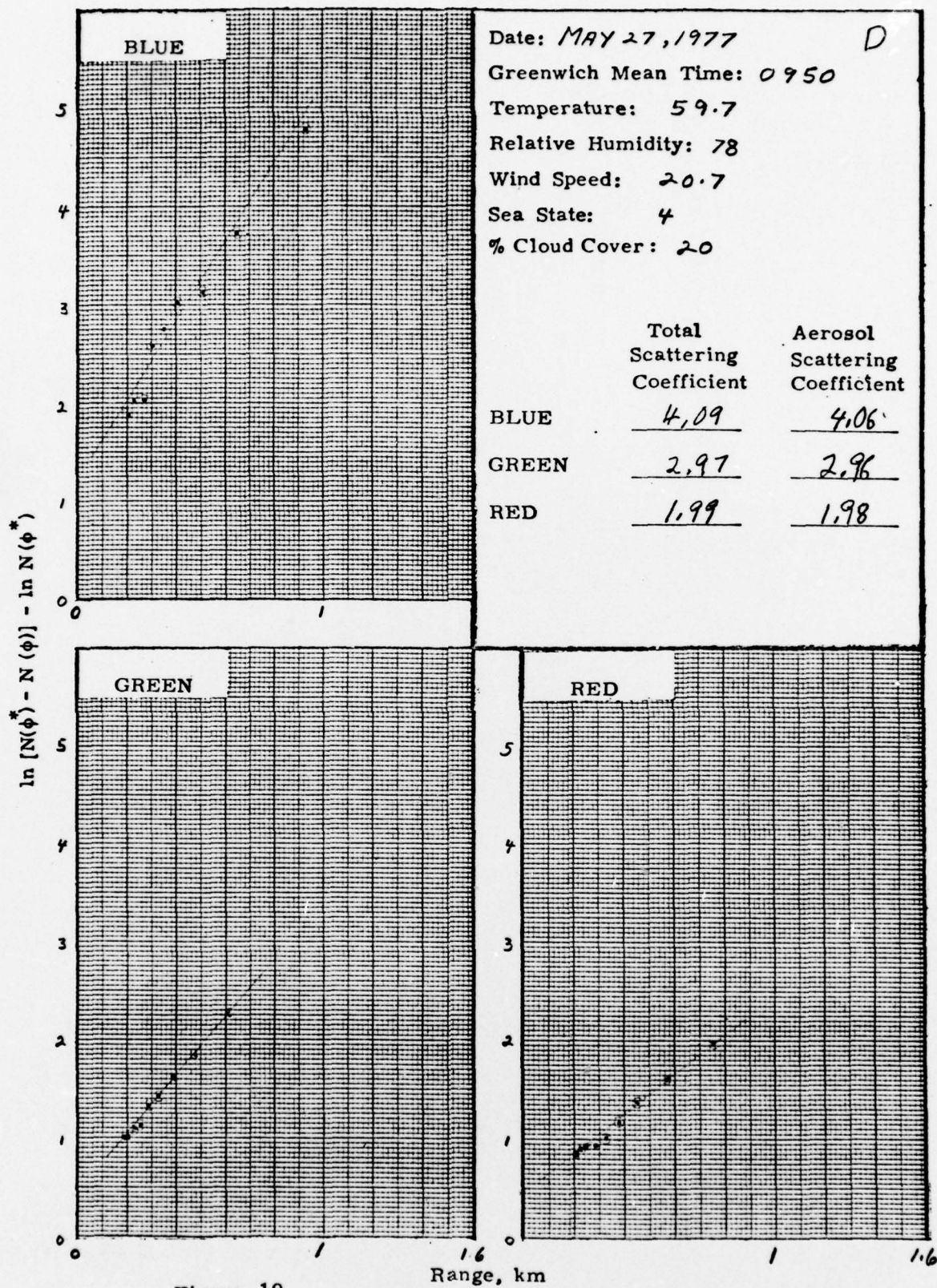


Figure 19

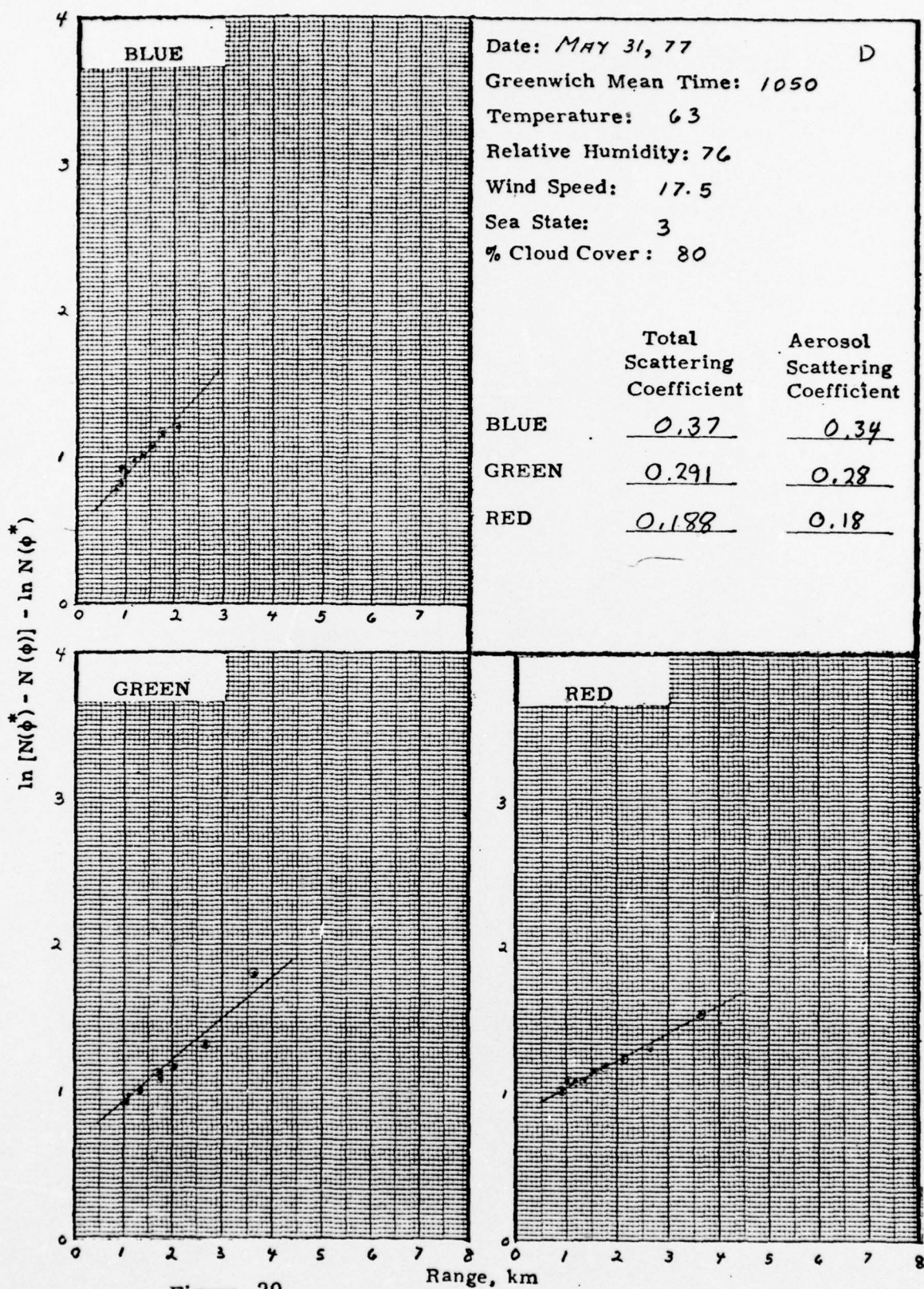


Figure 20

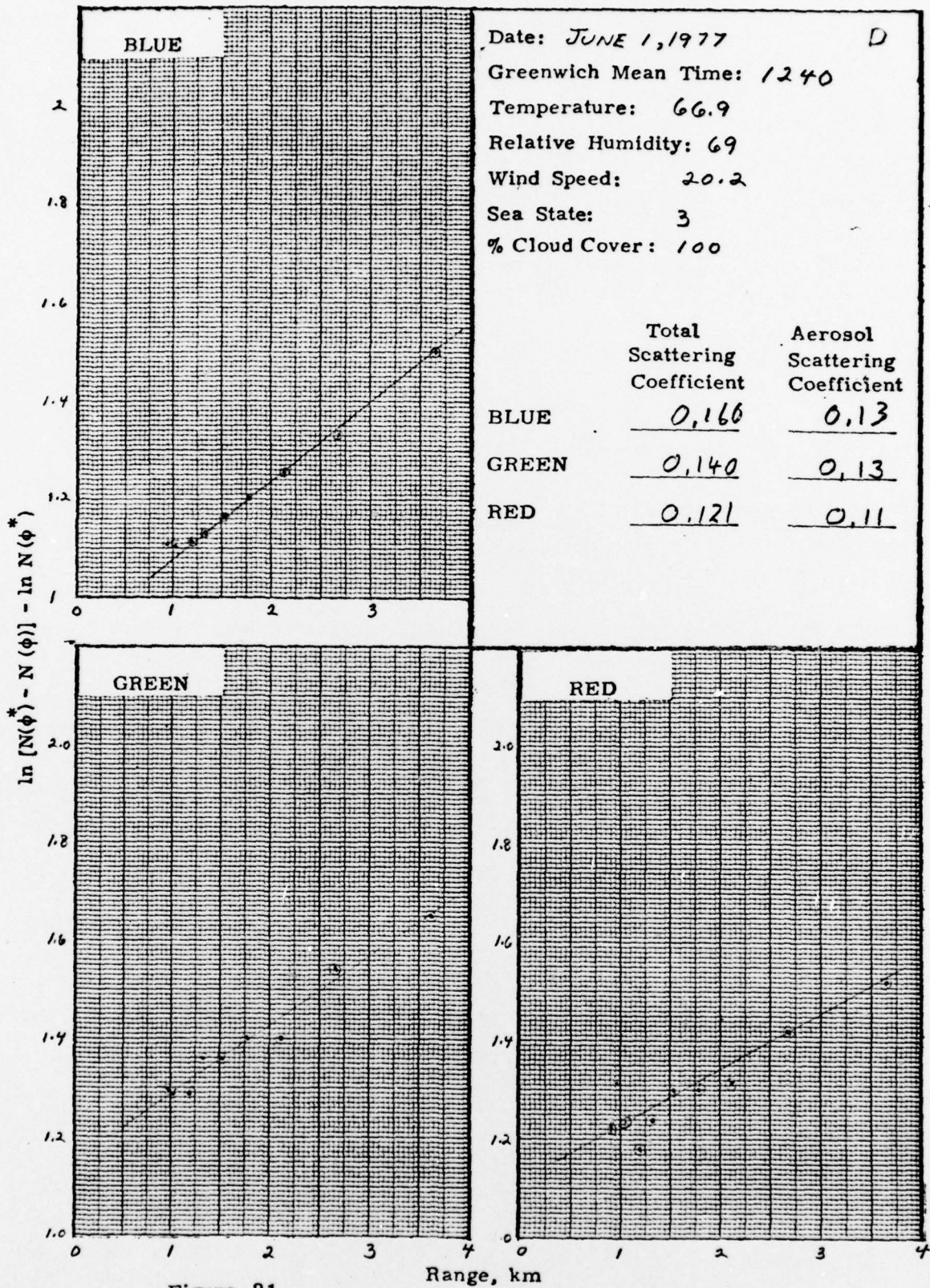


Figure 21

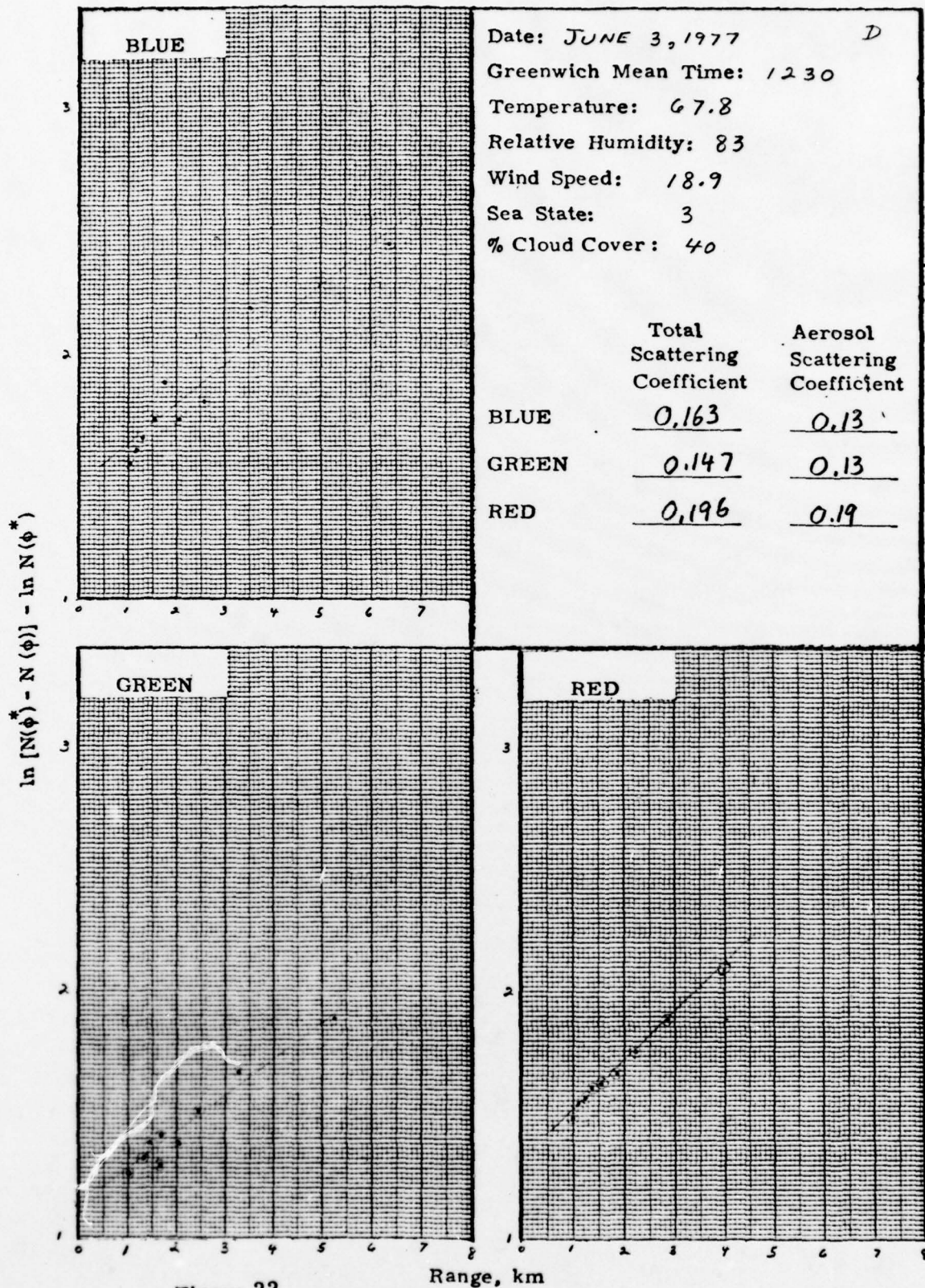


Figure 22

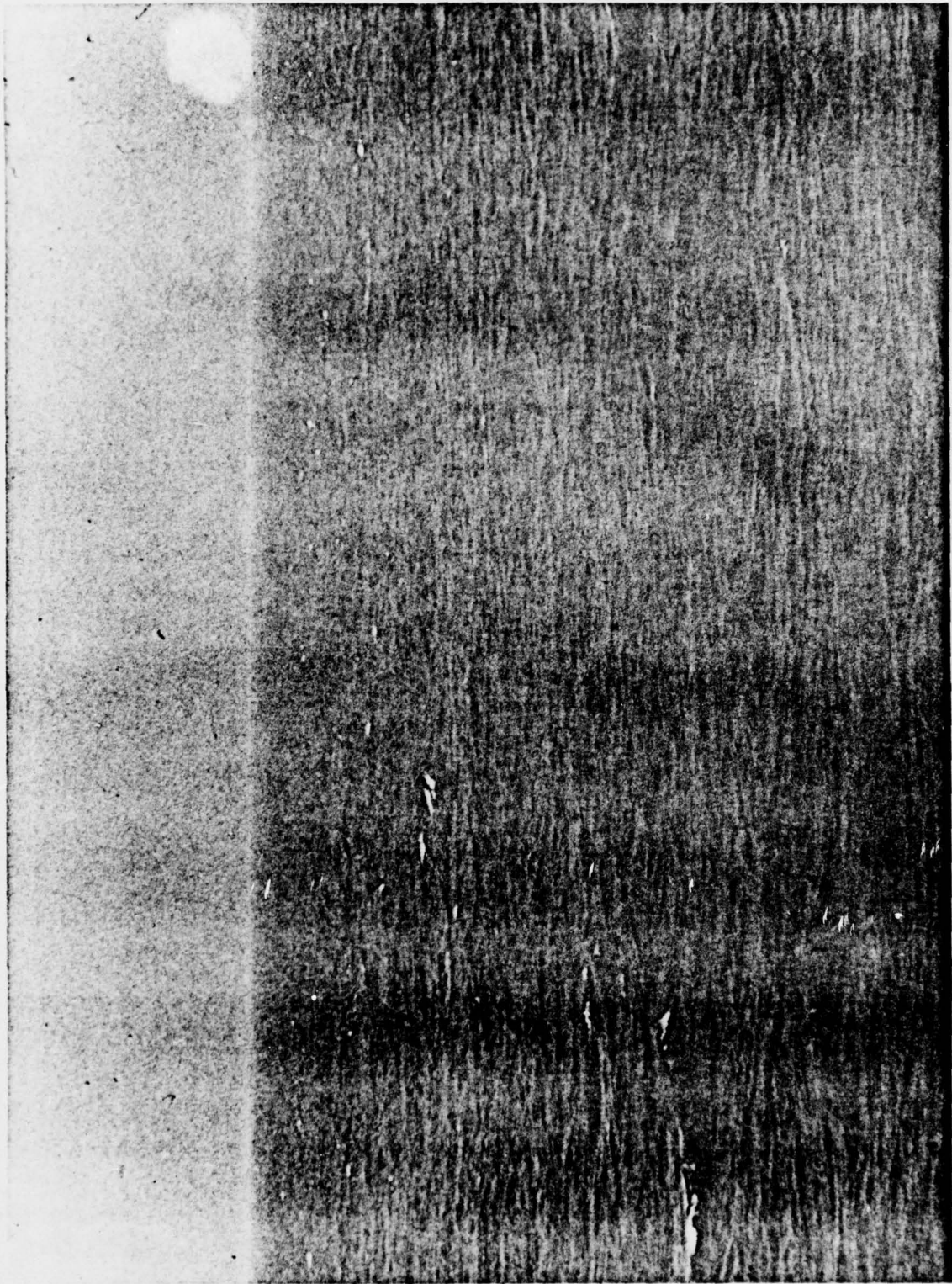


Figure 23. June 3, 1977 Time 1230, EOMET Film 16 FR16 Segment 3.

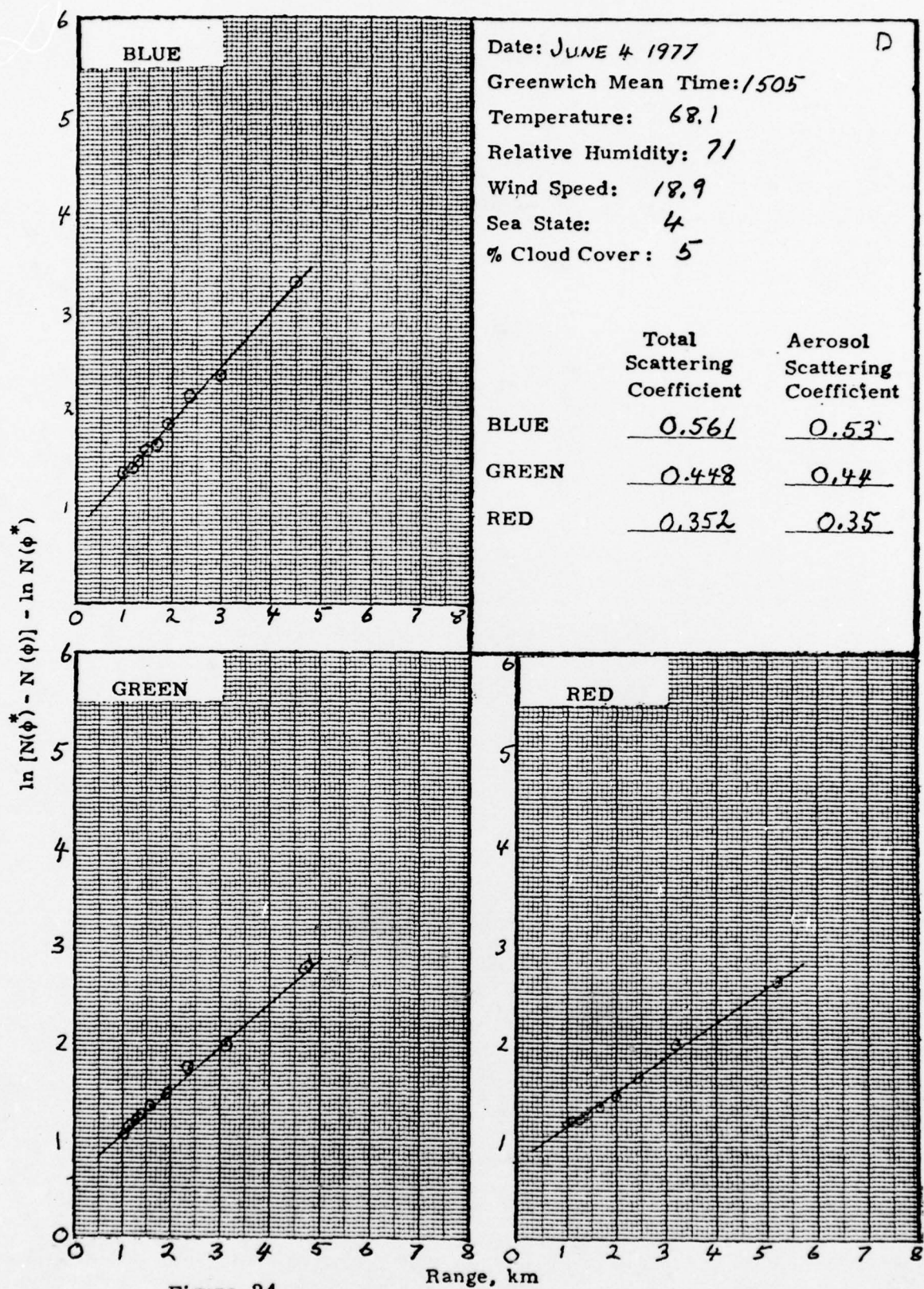


Figure 24.

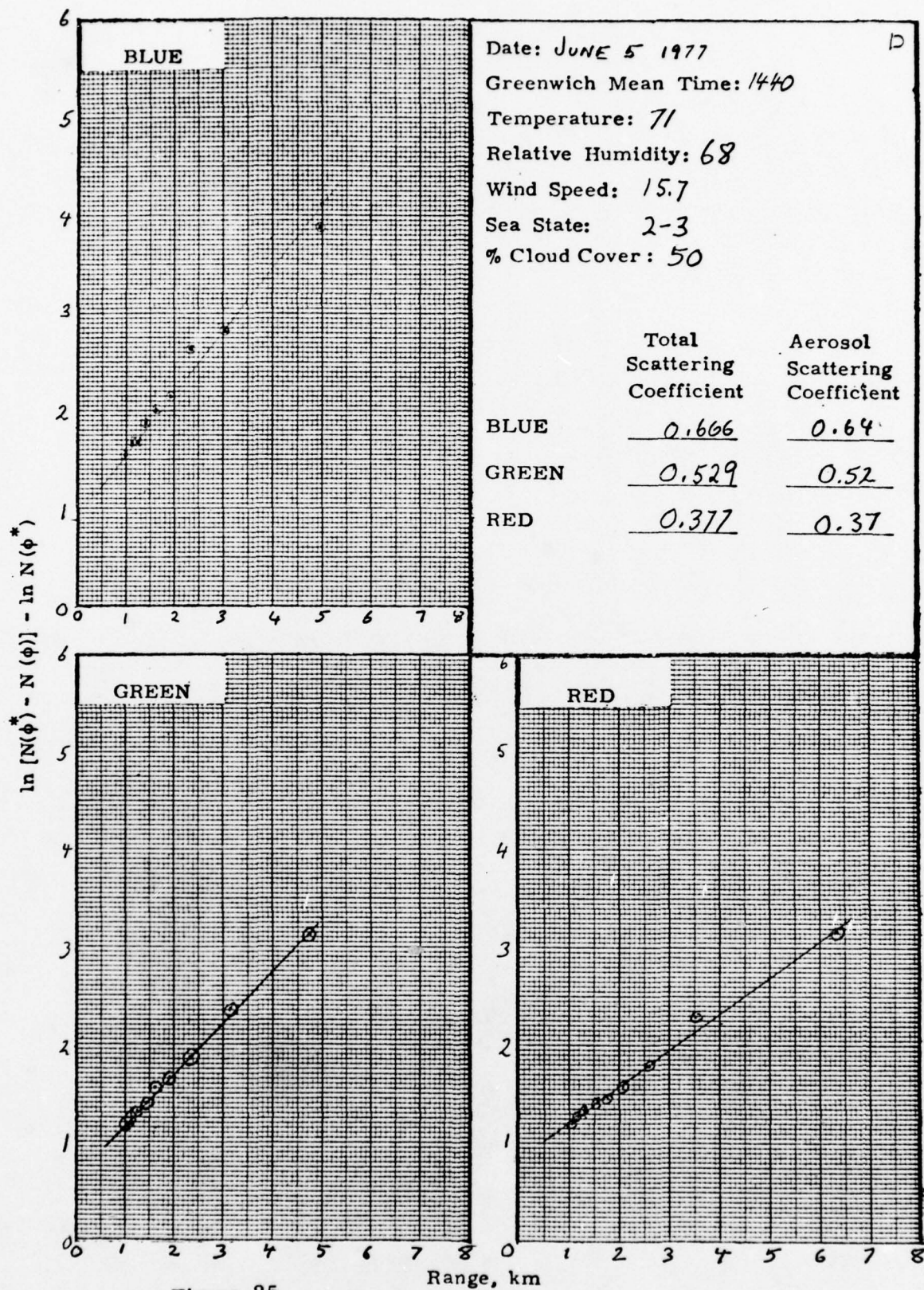


Figure 25.

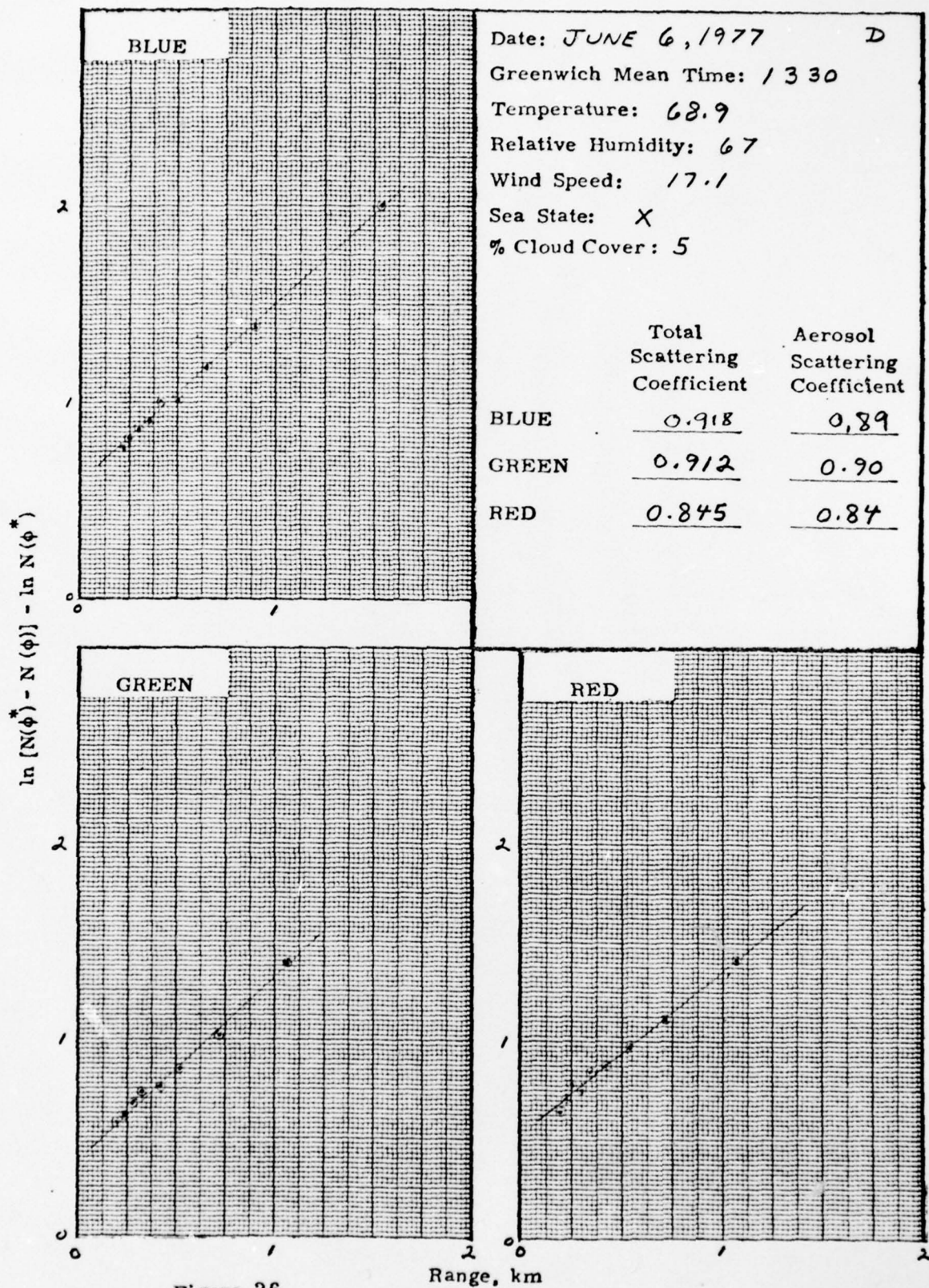


Figure 26.

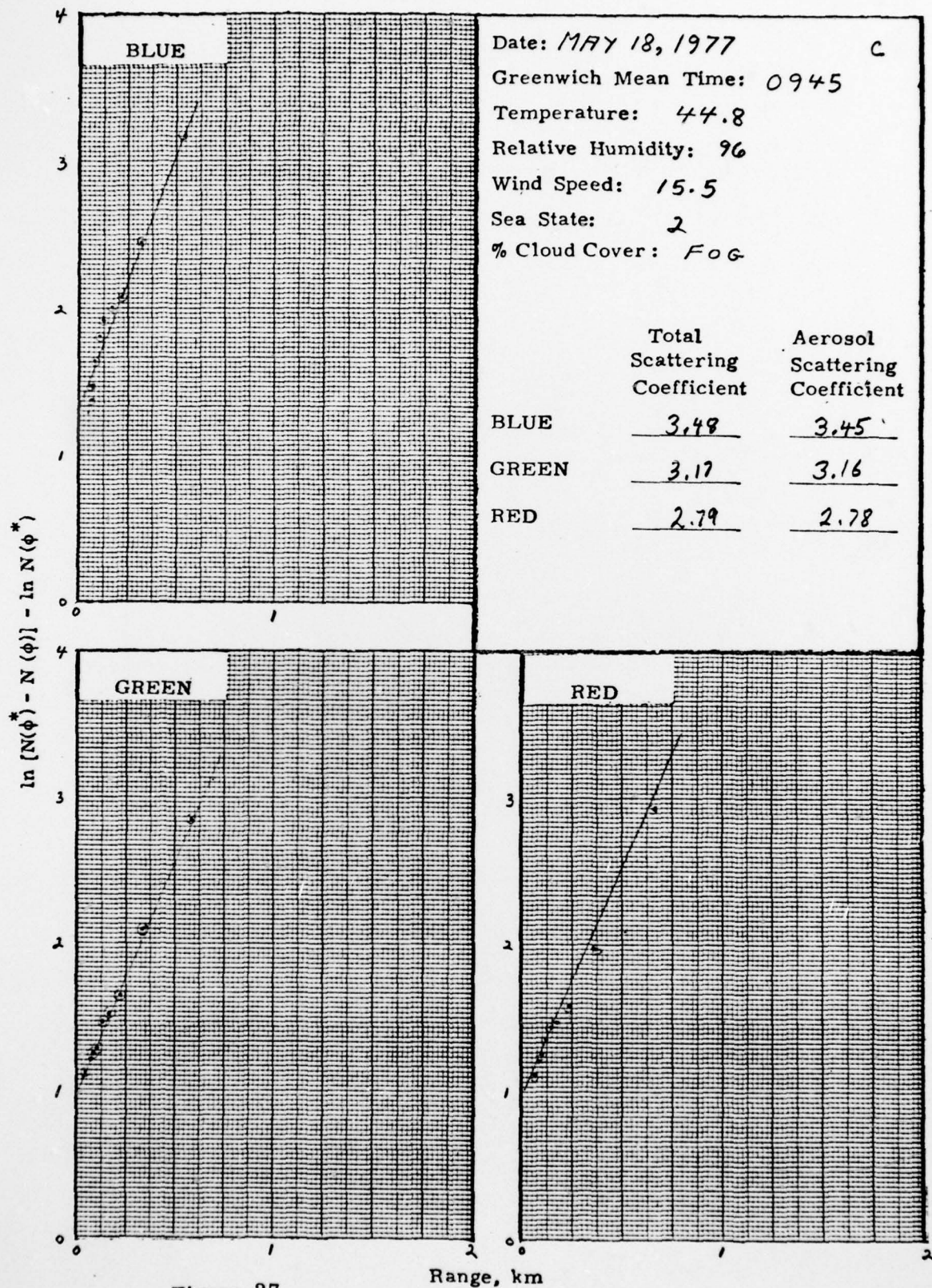


Figure 27.

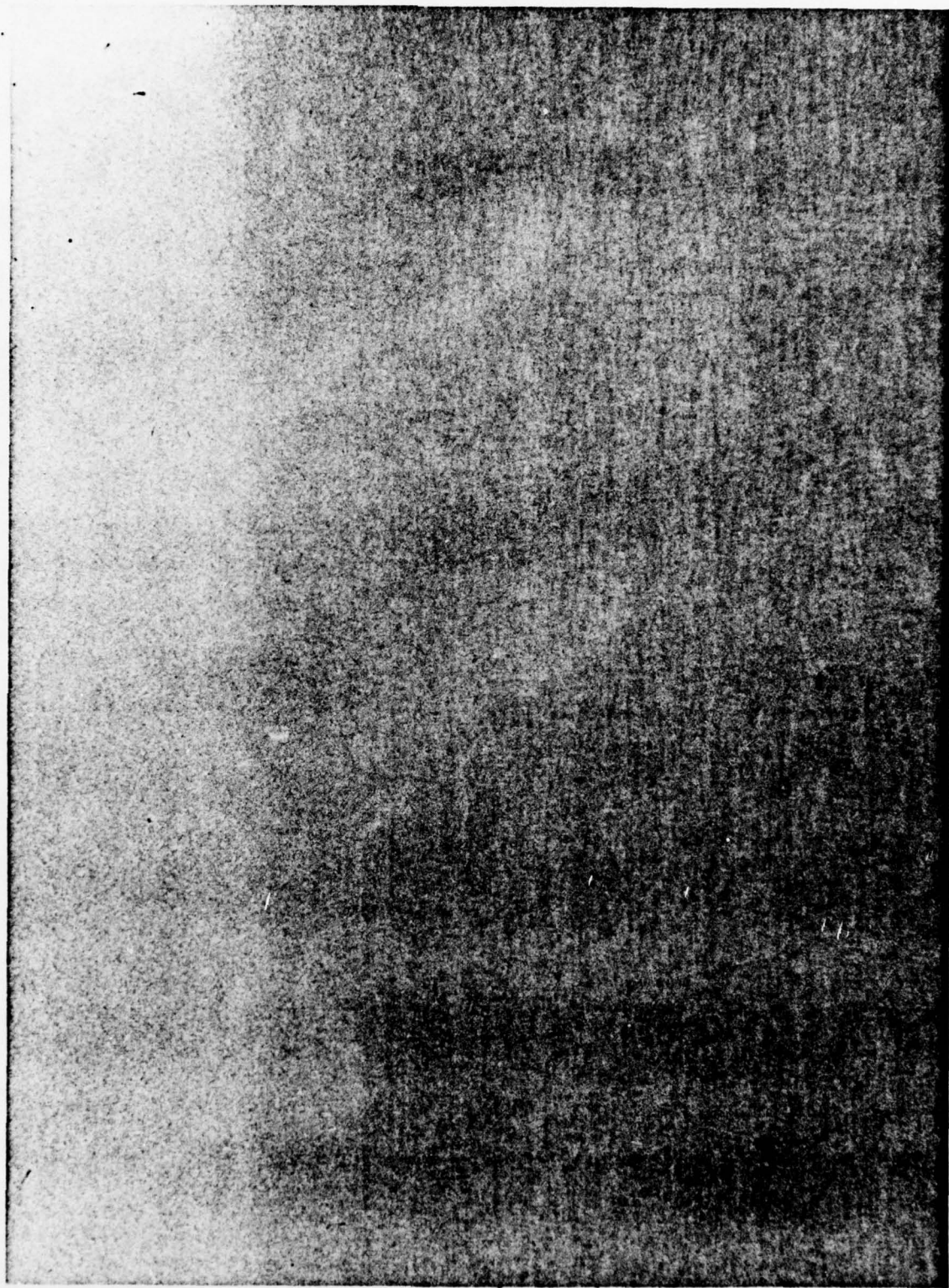


Figure 28. May 18, 1977 Time 0945. EOMET FR15 Film 2 Segment 3.

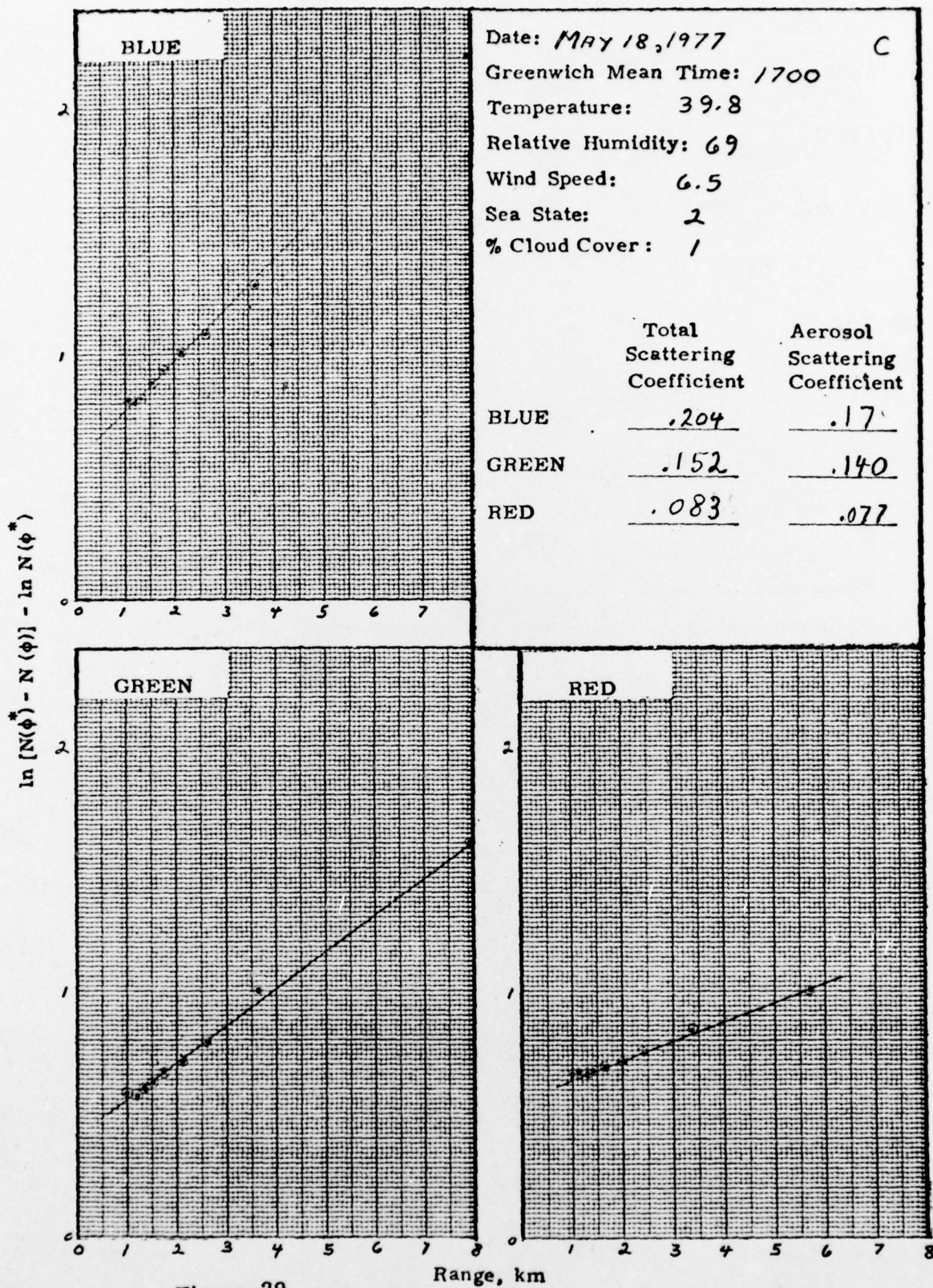


Figure 29

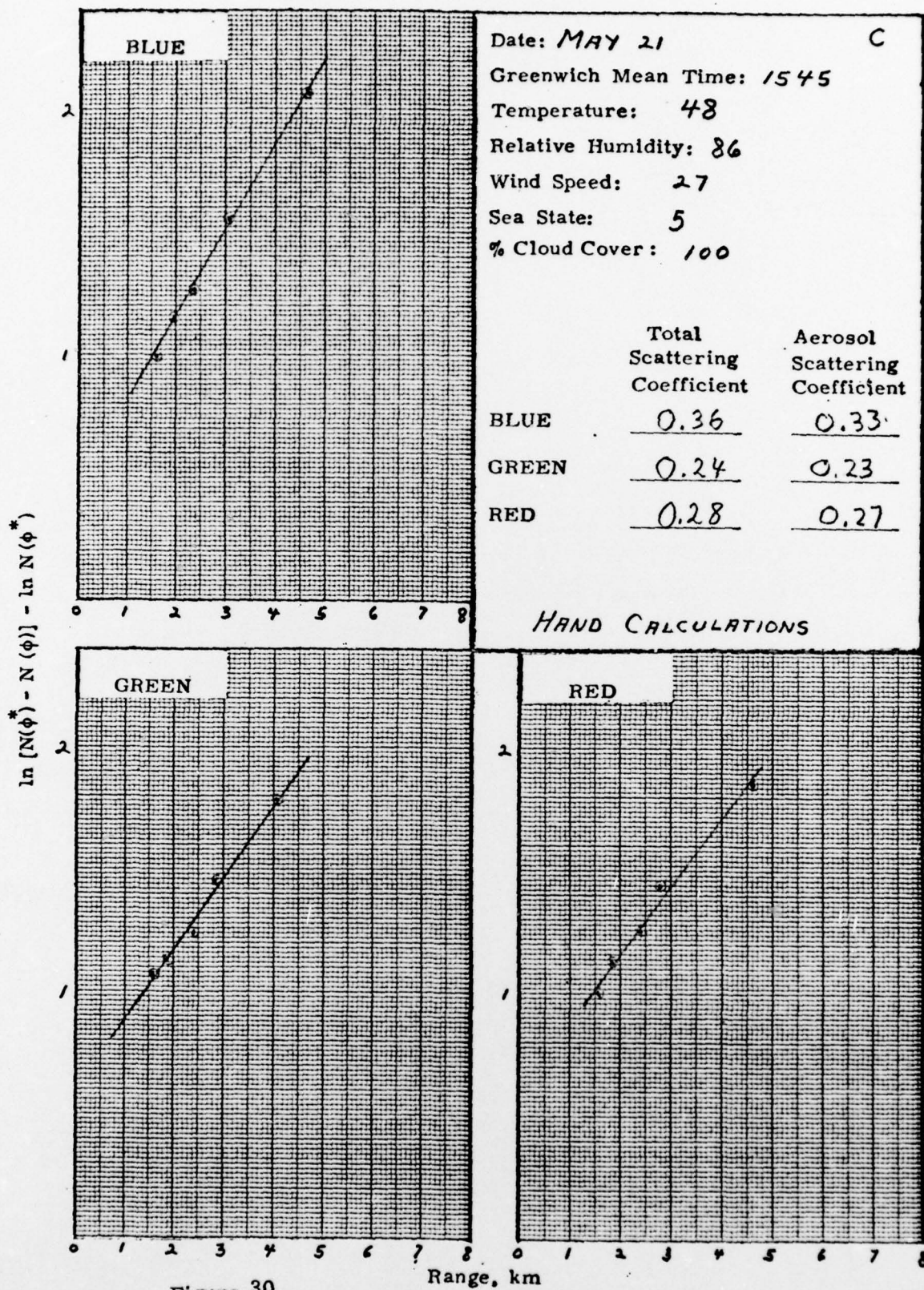


Figure 30.

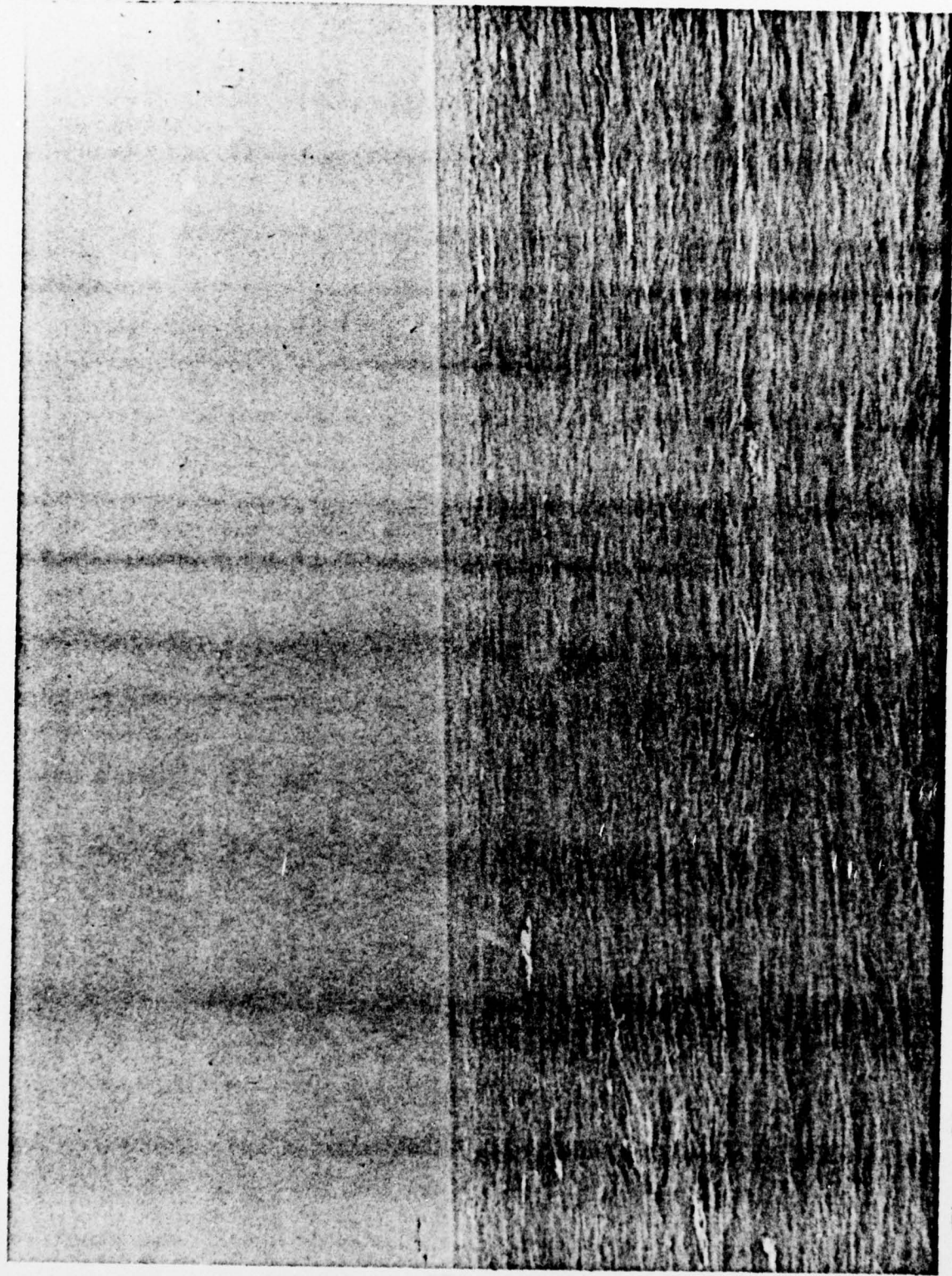


Figure 31. May 21, 1977 Time 1545 EOMET Film 4 FR11 Segment 2.

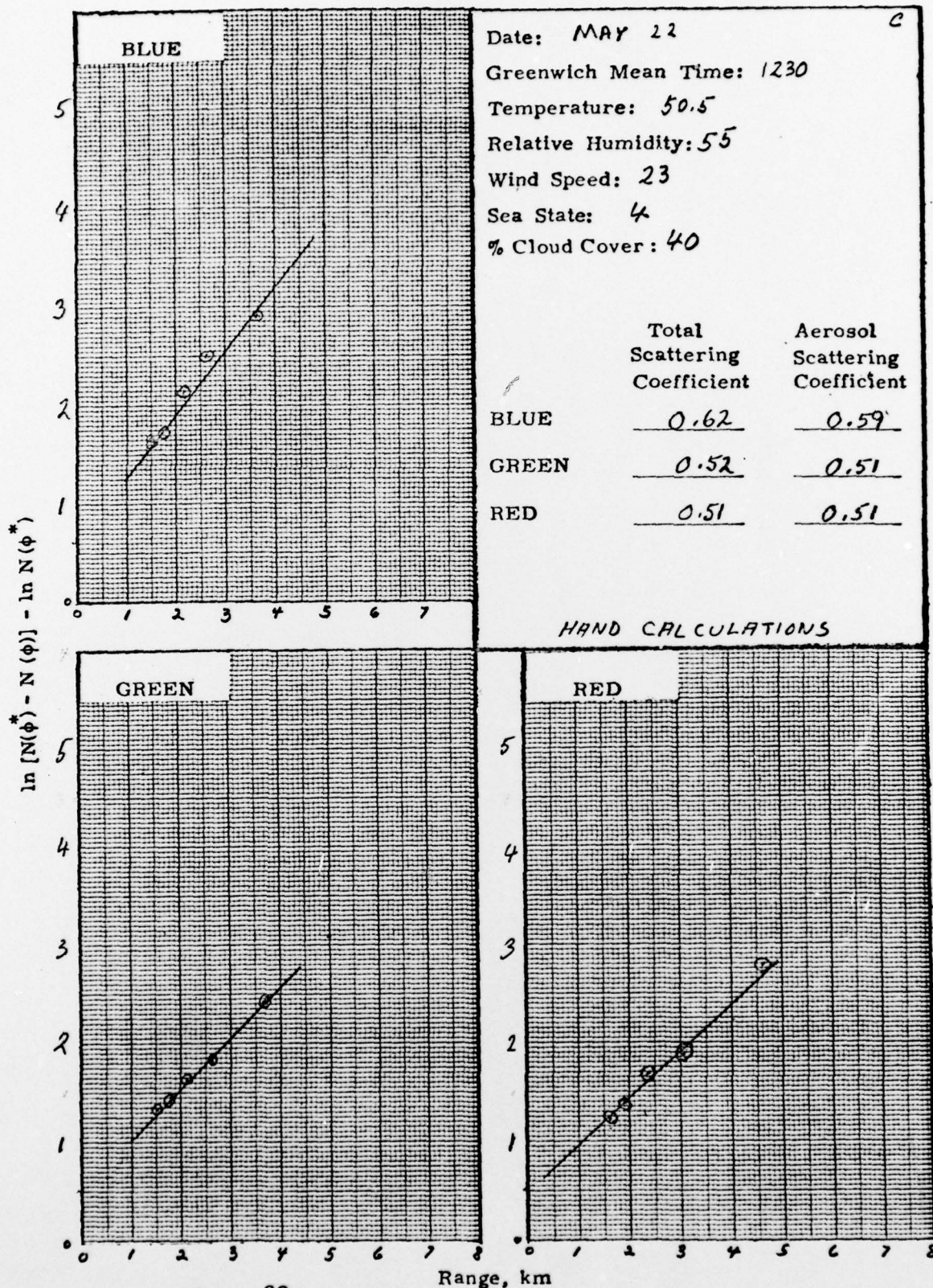




Figure 33. May 22, 1977 Time 1230 EOMET FR9 Film 5 Segment 2.

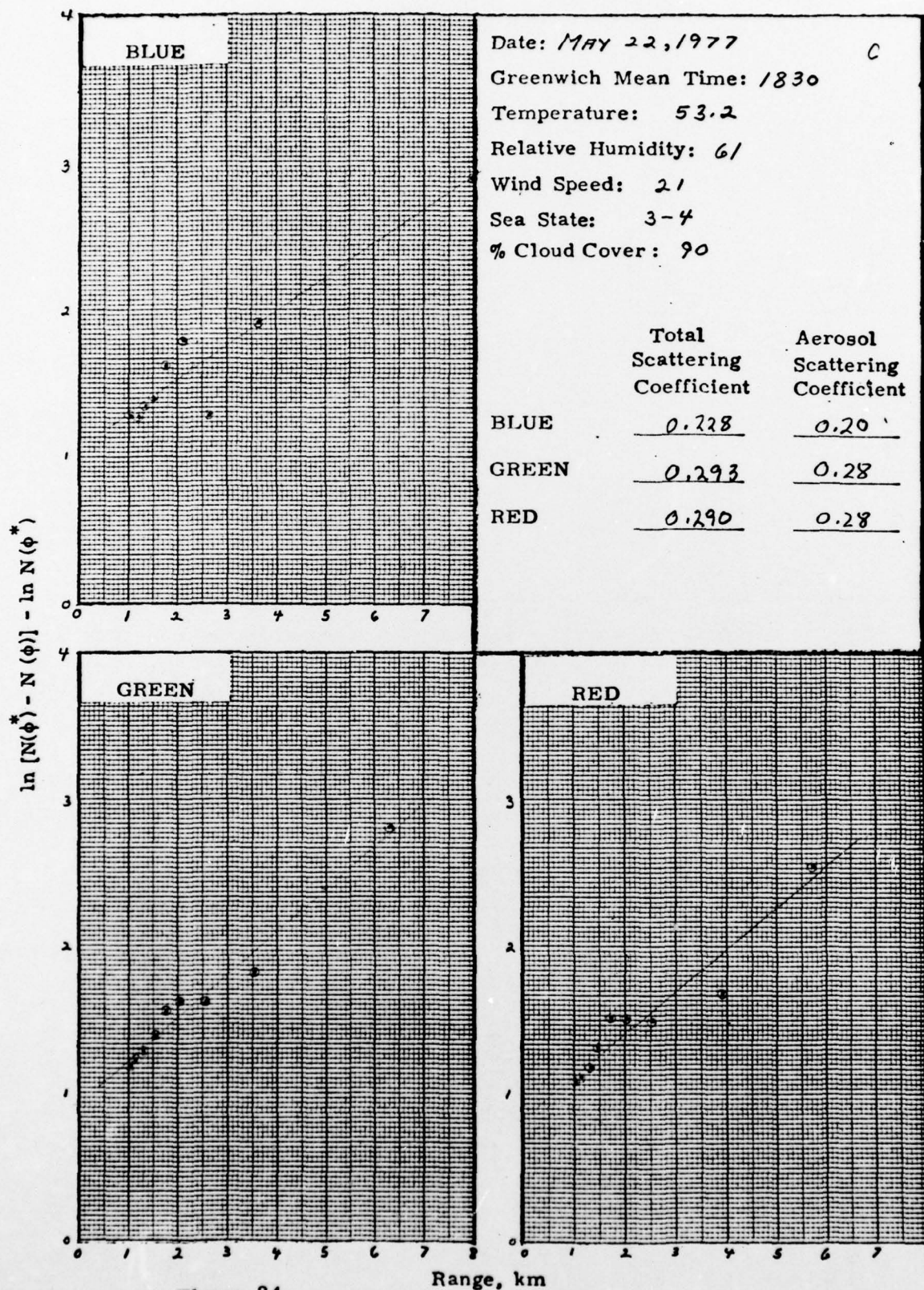


Figure 34.

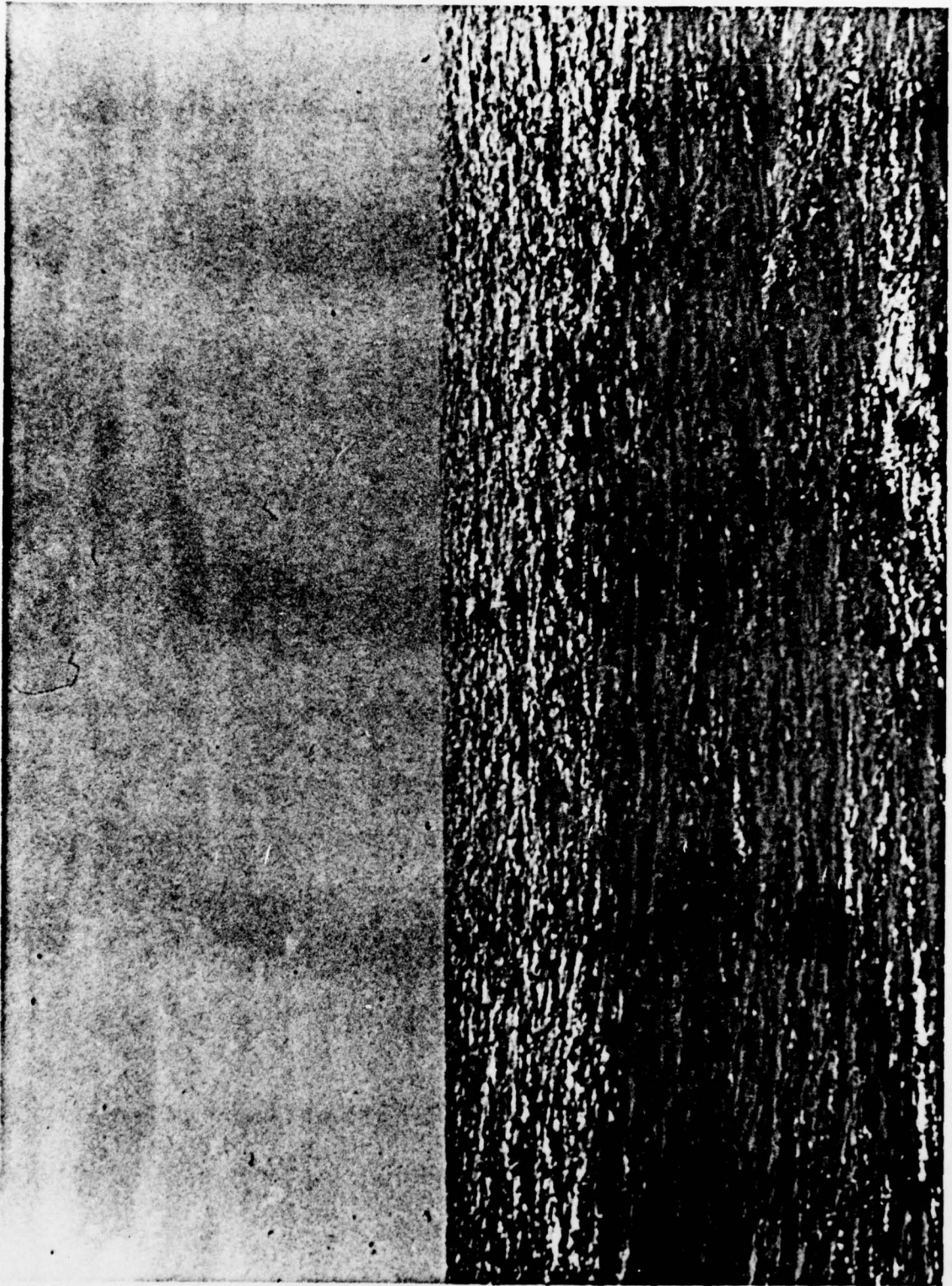


Figure 35. May 22, 1977 Time 1830 EOMET FR 10 Film 6 Segment 2.

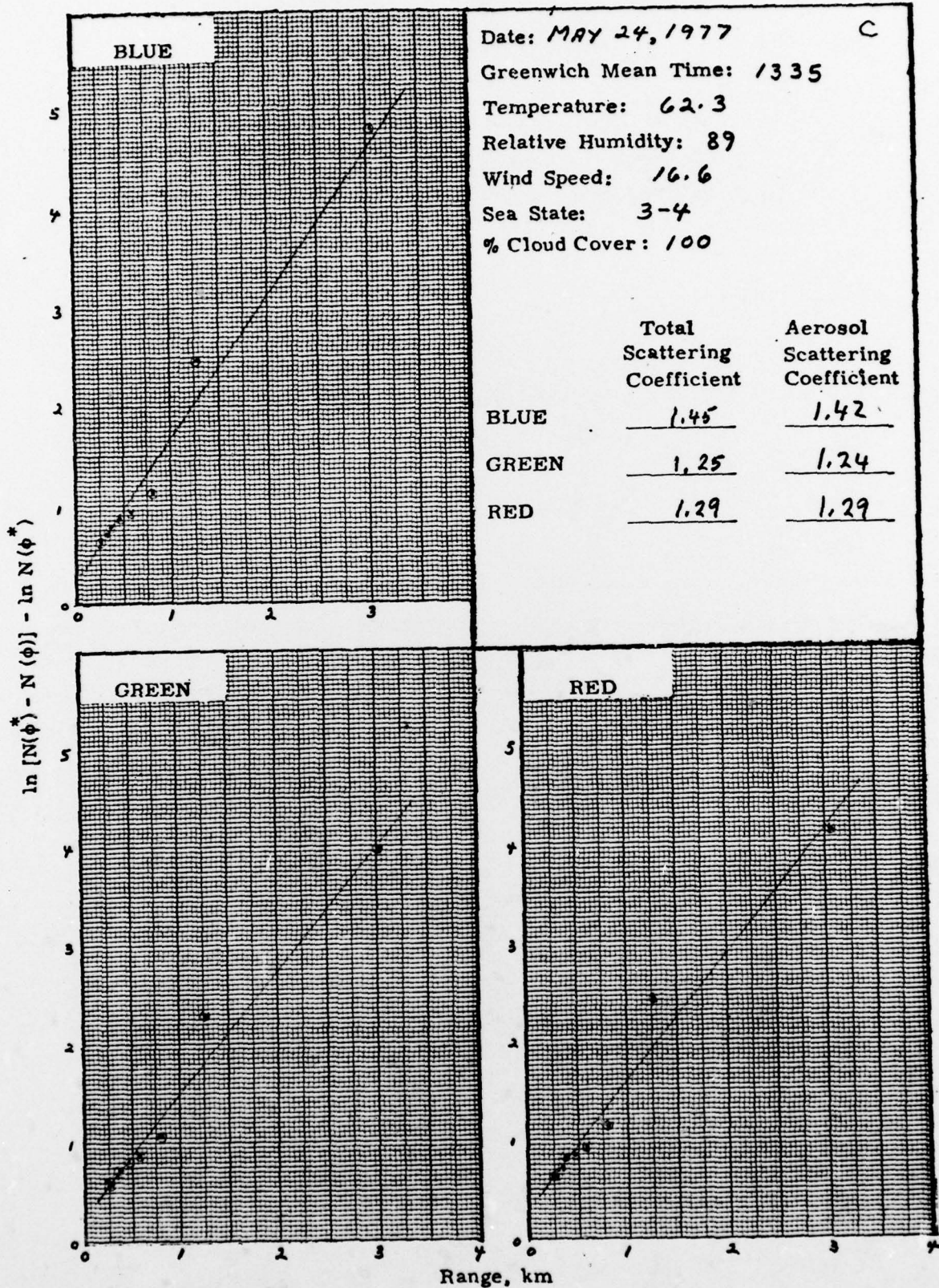


Figure 36.

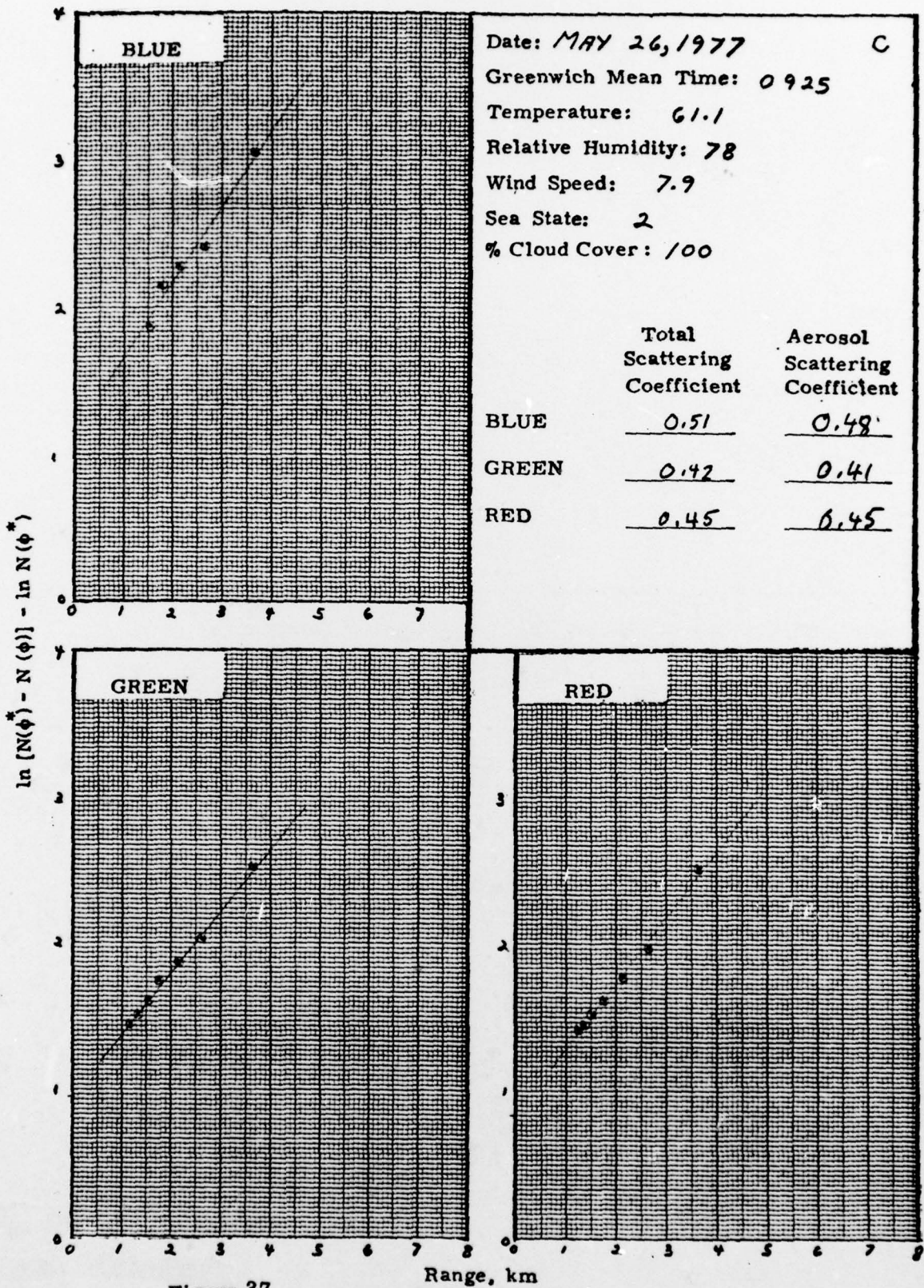


Figure 37.

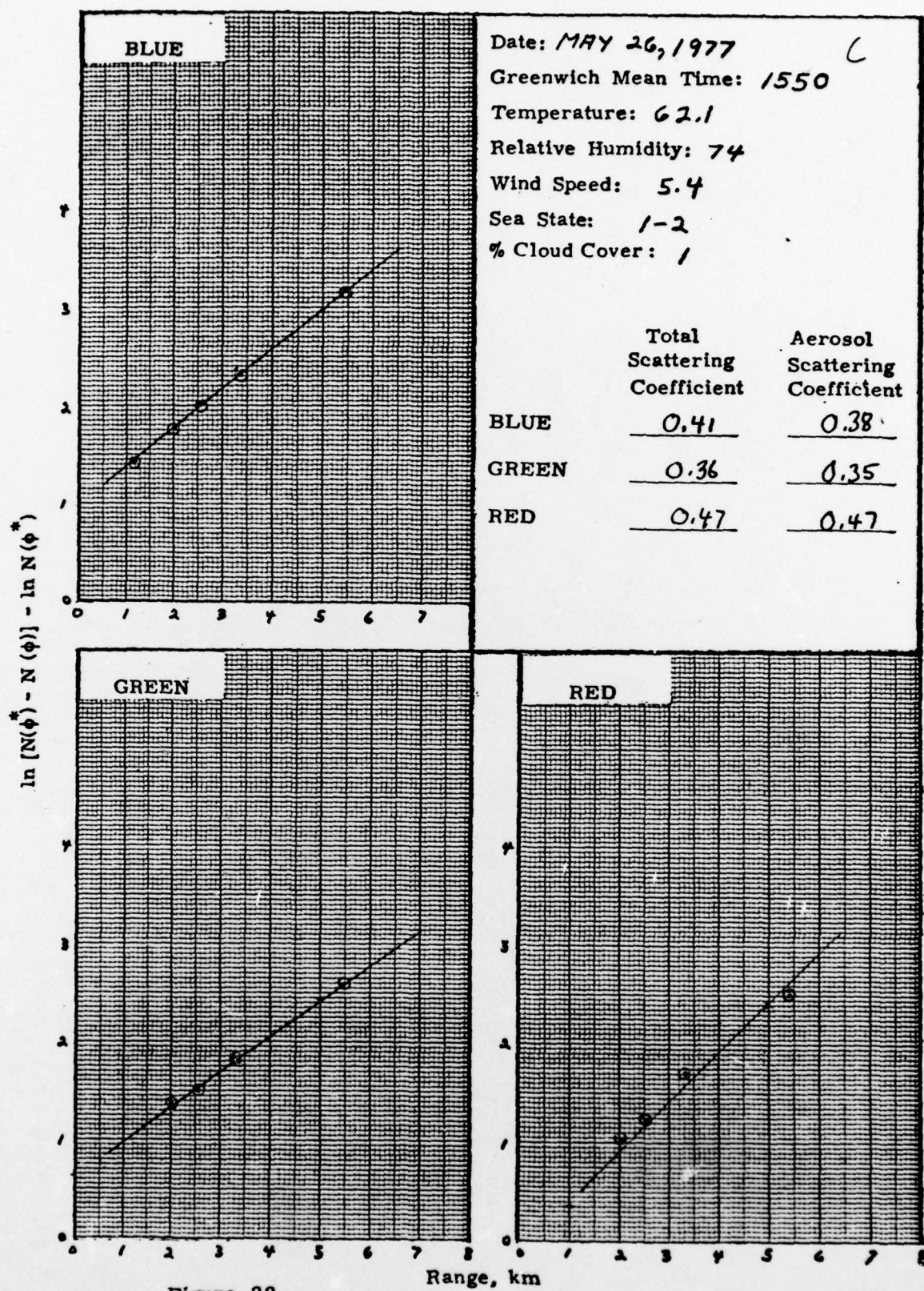
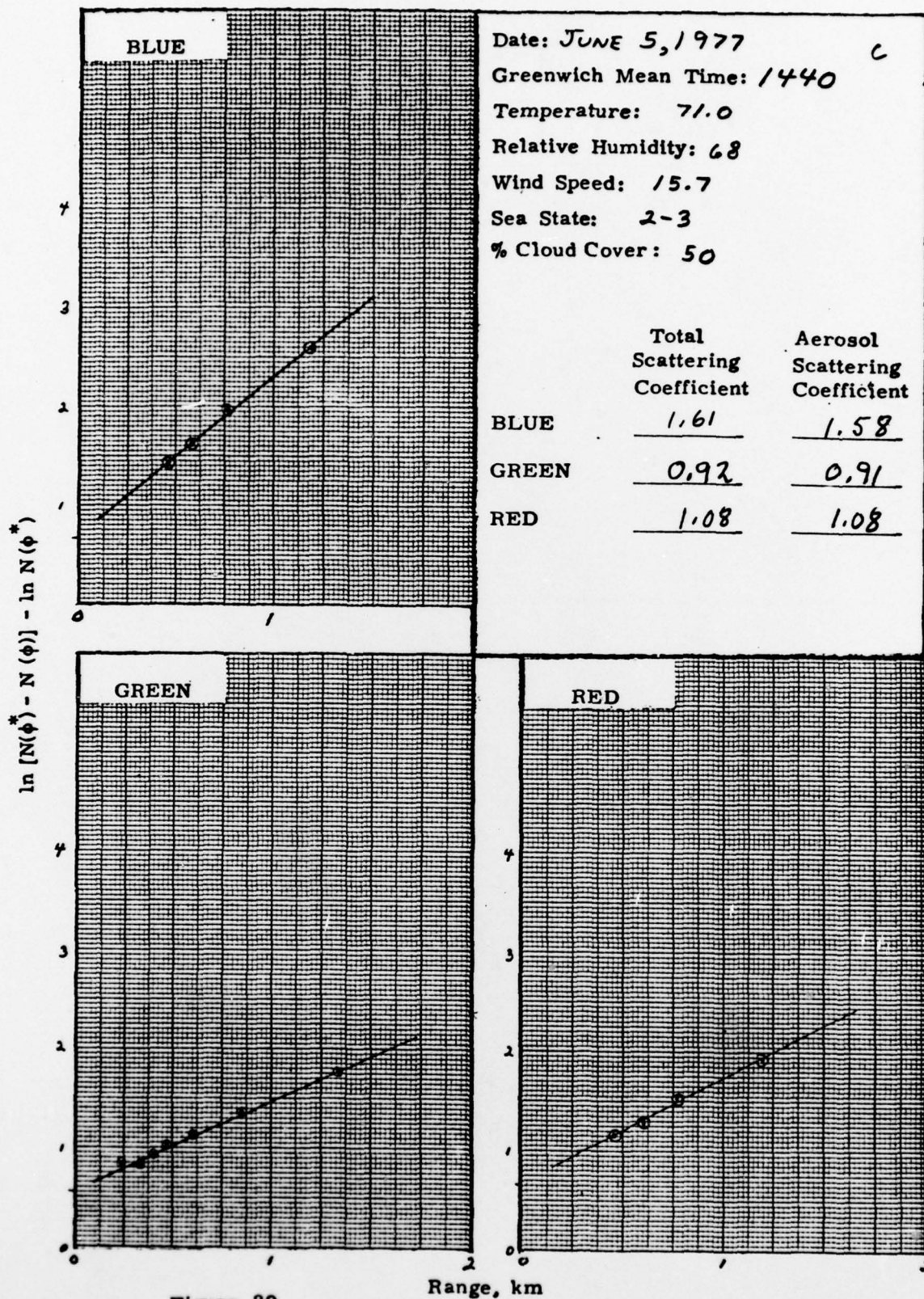


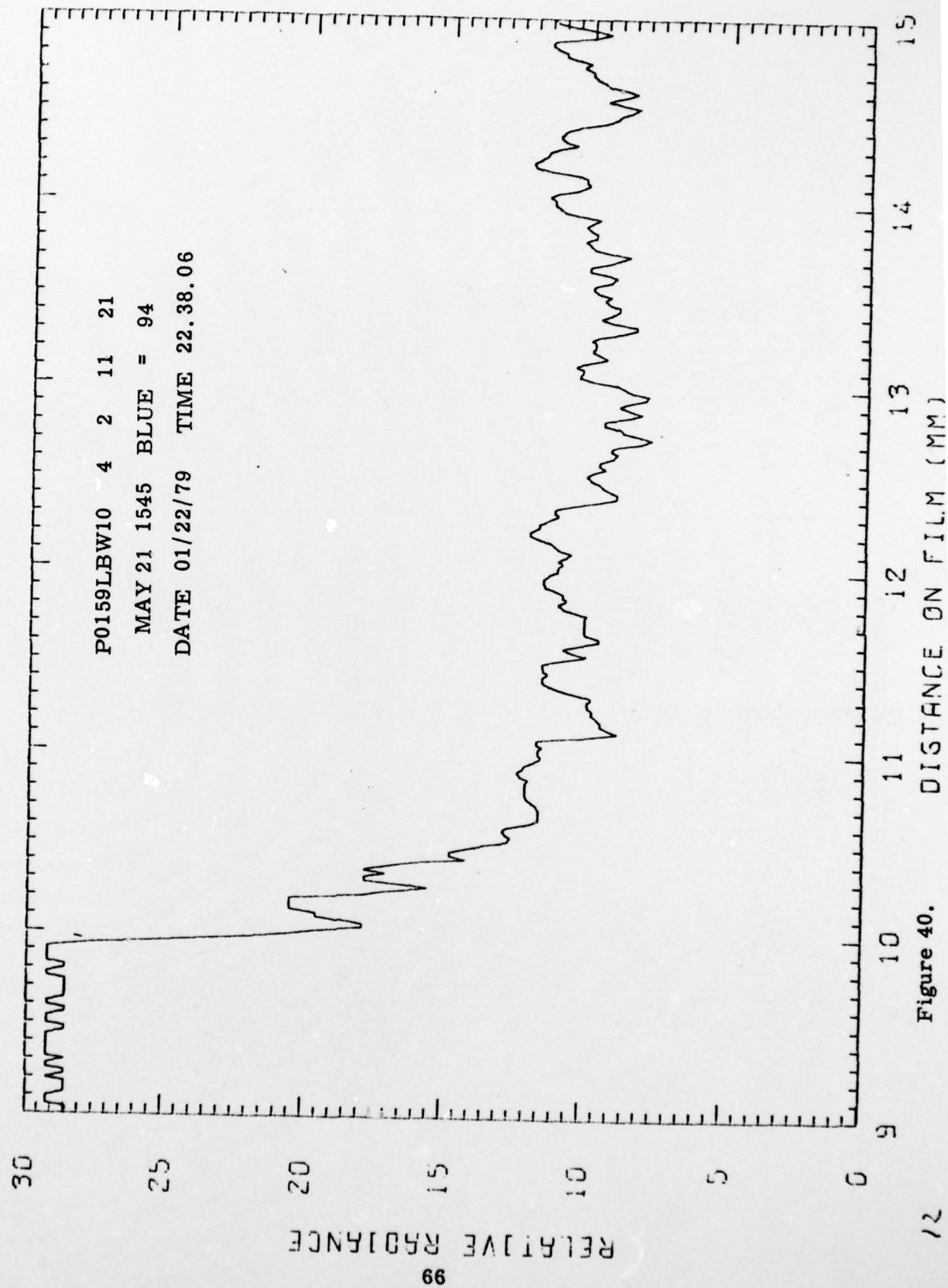
Figure 38.



Date: JUNE 5, 1977 C
 Greenwich Mean Time: 1440
 Temperature: 71.0
 Relative Humidity: 68
 Wind Speed: 15.7
 Sea State: 2-3
 % Cloud Cover: 50

	Total Scattering Coefficient	Aerosol Scattering Coefficient
BLUE	<u>1.61</u>	<u>1.58</u>
GREEN	<u>0.92</u>	<u>0.91</u>
RED	<u>1.08</u>	<u>1.08</u>

Figure 39



DISTRIBUTION

Naval Research Laboratories
Washington, D. C. 20375

Code: 8327 2/1
Attn: S. Gathman

Code: 2627 2/0
Attn: Tech Library

Defense Documentation Center
Bldg 5, Cameron Station
Alexandria, VA 22314

DODAAD Code SA 7031 12/0

HSS Inc 4/0
2 Alfred Circle
Bedford, Ma 01730